

# THEORETICAL MODELS OF PLASTIC DEFORMATION PROCESSES IN NANOCRYSTALLINE MATERIALS

M.Yu.Gutkin<sup>1</sup>, I.A.Ovid'ko<sup>1</sup> and C.S.Pande<sup>2</sup>

<sup>1</sup> Institute of Problems for Mechanical Engineering, Russian Academy of Sciences,  
Bolshoj 61, Vas. Ostrov, St.Petersburg, Russia

<sup>2</sup> Naval Research Laboratory, Washington, DC 20375, USA

Received: September 3, 2001

**Abstract.** We provide an overview of theoretical models of plastic deformation processes in nanocrystalline materials. The special attention is paid to the abnormal Hall-Petch relationship which manifests itself as the softening of nanocrystalline materials with reducing the mean grain size. Theoretical models are considered which describe the deformation behavior of nanocrystalline materials as two-phase composites with grain interiors and boundaries playing the role as component phases. Also, physical mechanisms (lattice dislocation motion, grain boundary sliding, diffusion plasticity mechanisms) of plastic flow in nanocrystalline materials are analysed with emphasis on transitions from one to another deformation mechanism with the reduction of grain size. The effect of a distribution of grain size on the abnormal Hall-Petch relationship in nanocrystalline materials is considered.

## 1. INTRODUCTION

Nanostructured materials represent a new generation of advanced materials exhibiting unique and technologically attractive properties due to the size and interface effects, e.g., [1-12]. The potential for nanostructured materials to transform so many technologies is almost without precedent. Of the special importance are the outstanding mechanical properties of nanocrystalline (nano-grained) materials, which are essentially different from those of conventional coarse-grained polycrystals. Nanocrystalline materials exhibit extremely high strength and good fatigue resistance [11-13] desired for numerous applications. At the same time, many nanocrystalline materials are rather ductile. In particular, nanocrystalline ceramics exhibit superplasticity commonly at lower temperatures and faster strain rates than their coarse-grained counterparts [14,15].

One of the specific features of deformation processes in nanocrystalline materials manifests itself in deviations from the known grain size scaling relations. The classic Hall-Petch relationship [16,17] describes the relationship between yield stress  $\tau$  and grain size  $d$  of a polycrystalline material, viz.,

$$\tau = \tau_0 + kd^{-1/2}, \quad (1)$$

where  $\tau_0$  is the friction stress considered needed to move individual dislocations, and  $k$  is a constant (often referred to as the Hall-Petch slope and is material dependent). This equation is well behaved for grains larger than about a micron. Masumura *et al* [18] have plotted some of the available data in a Hall-Petch plot. It is seen that the yield stress-grain size exponent for relatively large grains appears to be very close to -0.5 and generally this trend continues until the very fine grain regime (~ 100 nm) is reached. With the advent of nanocrystalline materials whose grain sizes are of nanometer (nm) dimensions, the applicability and validity of Eq. (1) becomes of interest in view of recently compiled experimental results [19].

A close analysis of experimental Hall-Petch data in a variety of materials shows three different regions: (1) a region from single crystal to a grain size of about a micron ( $\mu$ ) where the classical Hall-Petch description can be used; (2) a region for grain sizes ranging from about a  $\mu$  to about 30 nm where the Hall-Petch relation roughly holds, but deviates from the classical -0.5 exponent to a value near zero; and (3) a region beyond a very small critical grain

size where the Hall-Petch slope is nearly zero with no increase in strength on decreasing grain size or where the strength actually decreases with decreasing grain size. Although some of the measurements on which the trend discussed above is based on are not entirely reliable because of a variety of reasons discussed recently by Sanders *et al* [20], the above delineation into three regions is beginning to be accepted.

The specific peculiarities of the grain size dependency of the yield stress in nanocrystalline materials are definitely caused by their structural peculiarities which are the nano-scale structure and the extremely high volume fraction of the grain boundary phase. In this context, an adequate theoretical description of the grain size dependency of the yield stress in nanocrystalline materials, on the one hand, will essentially contribute to understanding the fundamentals of «structure-properties» relationships in nano-scale solids and, on the other hand, will serve as a basis for development of high technologies exploiting the outstanding mechanical properties of nanocrystalline materials.

At present, the nature of the deviations from the conventional Hall-Petch grain size scaling relation in nanocrystalline materials is the subject of controversy. In general, theoretical models of the phenomenon discussed can be divided into the two basic categories: (i) models describing nanocrystalline materials as two-phase composites with grain interiors and boundaries playing the role as component phases; and (ii) models describing evolution of defects and grain boundary structures, with focuses placed on physical mechanisms (lattice dislocation motion, grain boundary sliding, diffusion plasticity mechanisms) of plastic flow in nanocrystalline materials. The models of category (i) operate with the averaged mechanical characteristics and volume fractions of the grain-interior and grain-boundary phases. The models of the category (ii) deal with the nano-scale effects on conventional lattice motion and the competition between various deformation mechanisms and the effects of a distribution of grain size on this competition in nanocrystalline materials. The main aim of this paper is to provide an overview of the theoretical models of plastic deformation processes in nanocrystalline materials with the particular attention being paid to the abnormal Hall-Petch relationship.

Let us briefly characterize the basic aspects of the theoretical models describing the grain size dependency of the yield stress in nanocrystalline materials. All the models exploit the key structural

peculiarities of nanocrystalline materials – the nano-scale structure and the high volume fraction of the grain boundary phase – as input in analysis of the deformation behavior of such materials. In doing so, the models of different categories use different theoretical methods for a description of plastic deformation and distinguish different structural peculiarities as those playing the crucial role in plastic deformation processes in nanocrystalline materials.

Several models exploit the idea on lattice dislocation motion in grain interiors as the basic deformation mechanism in nanocrystalline materials, which is modified (compared to that in coarse-grained polycrystals) due to nano-scale effects. At the same time, the generic idea of the most models is that the grain boundary phase provides the effective action of deformation mechanism(s) in nanocrystalline materials, which is (are) different from the lattice dislocation mechanism realized in conventional coarse-grained polycrystals. In context of this generic idea, the dominant role of the lattice dislocation mechanism causes the grain refinement to strengthen a coarse-grained material (Fig. 1a), in which case a classical Hall-Petch relationship is valid. At the same time, when the deformation mechanisms associated with the active role of grain boundaries effectively come into play (Fig. 1b), the grain refinement will weaken a specimen; it is the case of nanocrystalline materials. The theoretical models under consideration are distinguished by their identification of the deformation mechanism(s) inherent to grain boundaries and their description of the competition between these mechanisms and the conventional lattice dislocation motion. The following plastic deformation mechanisms commonly are treated as those associated with the active role of grain boundaries and the nano-scale structure, effectively competing with the lattice dislocation mechanism in nanocrystalline materials: grain boundary sliding and diffusional mass transfer occurring predominantly via grain boundary diffusion.

The models of nanocrystalline materials as two-phase composites (models of the category (i)) describe their yield stress  $\tau$  and other mechanical characteristics with the help of the so-called rule of mixture. In this approach, the yield stress  $\tau$  of a nanocrystalline material is some weighted sum (mixture) of the yield stresses characterizing the grain-interior and grain-boundary phases, which strongly depends on the volume fraction of the grain boundary phase and, therefore, the grain size  $d$ . The yield stress of the grain-boundary phase is assumed to be lower than that of the grain-interior phase, in which case the rule of mixture describes

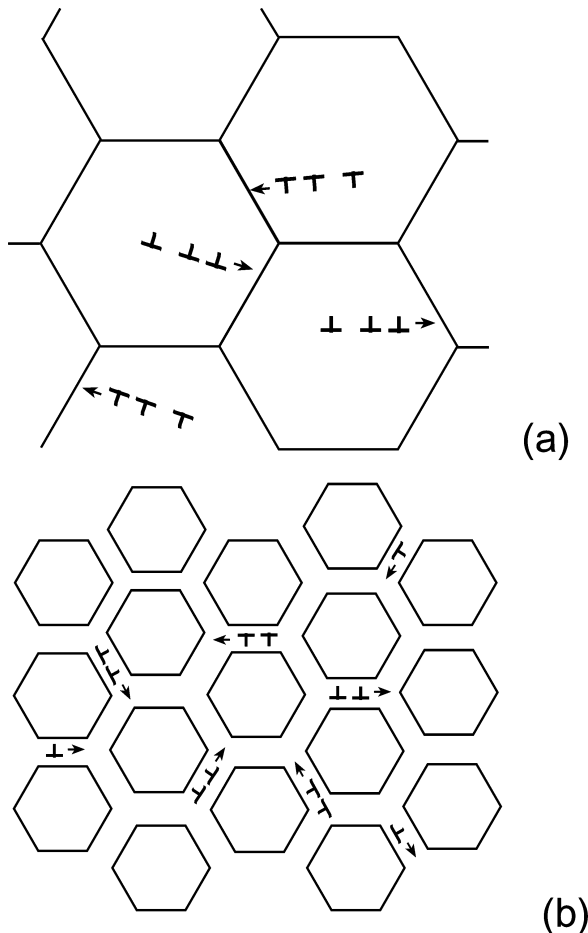


**Fig. 1.** Grain boundaries (a) play the role of obstacles for lattice dislocations in coarse-grained polycrystals and (b) serve as softening structural elements that carry plastic flow in nanocrystalline materials.

the deviations from the conventional Hall-Petch relationship in accordance with experimental data. Such models commonly do not take into account the evolution of defects and transformations of grain boundary structures, which, generally speaking, are capable of strongly influencing the deformation behavior of a mechanically loaded nanocrystalline material. The theoretical models based on the “rule-of-mixture” approach are reviewed in detail in section 2.

The theoretical models addressed the physical mechanisms of plastic flow in nanocrystalline materials focus on the evolution of defects (lattice dislocations, grain boundary dislocations, vacancies) being carriers of plastic flow and transformations of grain boundary structures, that accompany deformation processes in nanocrystalline materials. Such models belonging to the category (ii) often deal with a direct comparison of the characteristics of these

mechanisms. That is, the plastic deformation mechanism that requires less yield stress (or energy) is favoured, in which case the nanocrystalline material is characterized by yield stress inherent to the favoured deformation mechanism. A modified scheme of estimate of the yield stress is suggested in the approach taking into account a distribution of grain sizes occurring in most nanocrystalline specimens. This approach exploits the idea on the simultaneous action of various deformation mechanisms in various local areas of a mechanically loaded nanocrystalline material, depending on the grain size in such areas. In doing so, one operates with averaged (over a distribution of grain size) mechanical characteristics of nanocrystalline materials. We include into the category (ii) also the computer models describing physical mechanisms of plastic deformation in nanocrystalline materials and transitions from one to another deformation mechanism, occurring with reduction of the grain size  $d$ . All the above models are considered in section 3 of the review. Section 4 contains concluding remarks.

## 2. “RULE-OF-MIXTURE” APPROACH TO HALL-PETCH RELATION FOR NANOSTRUCTURED SOLIDS

The “rule-of-mixture” approach has become one of the widely spread ways to describe the Hall-Petch relation for nanostructured solids. The main idea of the simplest rule of mixture is that to estimate some macroscopic physical quantity which would describe a complex solid as a whole, they use an overall value equal to the sum of appropriate quantities for separate parts of the solid multiplied by volume fractions of the solid parts. More exact (but more complicated) rules of mixture take into account the geometry of mutual distribution of components within the solid as well as some their properties. Such theories of “effective” macroscopic overall properties are mostly developed in the science of composite materials (e.g., see [21,22]).

Kocks [23] probably was the first who decided to use the analogy between usual polycrystalline solids and composite materials. Indeed, disregarding mutual misorientations of grains, one can consider a polycrystalline solid as a composite which consists of single-crystalline matrix and intercrystalline layers (inclusions). Assuming the bulk areas of grains (matrix) are characterized by the yield stress  $\tau_g$  while the boundary layers of thickness  $t$  by the yield stress  $\tau_b$ , Kocks [23] used the rule of mixture and obtained the following estimate

$$\tau_y = \tau_G + \frac{4t}{d}(\tau_B - \tau_G) \quad (2)$$

for the yield stress  $\tau_y$  of a polycrystalline solid with grain size  $d$ . Obviously, the Hall-Petch relation is not attributed to the model [23] because Eq. (2) gives  $\tau_y \sim d^{-1}$  instead of the usual Hall-Petch law,  $\tau_y \sim d^{1/2}$ . It is worth noting, however, that this is true until the quantities  $\tau_G$  and  $\tau_B$  are treated as constants which do not depend on the grain size  $d$  themselves. We will consider below some models where this assumption is not satisfied at all or it is satisfied for  $\tau_B$  only. As was noted in the review [24], the Kocks' model [23] may only be correct for polycrystalline materials with very small grains. Really, Jang and Koch [25], trying to find the source of the spread in the results they obtained, discovered that the microhardness of nanocrystalline iron may follow the  $d^{-1}$  dependence as well as the  $d^{-1/2}$  dependence.

Kocks' idea to represent a polycrystalline material as a composite of a crystalline matrix with inclusions of intercrystalline layers was developed in the work by Gryaznov *et al* [26] aimed to obtain a generalized empirical analogue of Hall-Petch law and explain the reasons of its breaking for small grain sizes. Some deviations of the  $\tau_y(d)$  dependence from the usual Hall-Petch law were already observed in early experiments on microhardness measurement for nanocrystalline materials. For example, microhardness-test experiments performed with nanocrystalline Ni [27, 28], TiO<sub>2</sub> [29-31], Cu [28, 32-34] and copper alloys [35], Pd [32-34], Co [28], Fe [25, 36], Ag [37, 38], Ti-N [39] and Ni-Al [40] alloys, as well as multiphase alloys [41, 42] showed that only the 2-to-7-fold (for pure metals) and 2-to-4-fold (for multiphase alloys) increase in the yield stress  $\tau_y$  is observed for real materials instead of the hundred-fold increase in the value of  $\tau_y$  that is expected from the usual Hall-Petch law for materials with  $d$  as small as 10 nm. These experiments demonstrated that the value of  $\tau_0$  describing the lattice friction in the Hall-Petch relation, can increase [25], and the value of the Hall-Petch coefficient  $K$  can decrease [25,33] or even change sign [32, 36, 41-47].

Ten years ago, practically, there existed no theoretical models of the processes capable to lead up to the effects observed. Information on structure and properties of nanocrystalline materials and grain boundaries was very inconsistent. The question was actively discussed whether one should treat the state of material in grain boundaries as a new state of matter which can not be considered as crystalline or amorphous [48-54] because the state demon-

strated the total absence of even short translational order which is characteristic for both the amorphous and quasicrystalline states. In such a situation, when authentic data on the structure and mechanisms of plastic deformation in nanocrystalline materials were absent, it was decided to develop a generalized empirical analogue of Hall-Petch law which would allow for the yield characteristics of the materials of nanograins and intergranular layers, without dwelling on the particular physical processes that determine the yield stress in such materials [26].

Following Kocks [23], represent a nanocrystalline material as a composite of a single crystalline matrix with inclusions of intercrystalline layers. The experimental value of the ratio of typical sizes of crystallites and interfaces is large enough to consider the interfaces in the matrix as thin plates which are chaotically placed and oriented. As all the possible orientations of the inclusions are equally probable, a medium with isotropic effective properties can be considered. Representing the inclusions by oblate ellipsoids, the effective shear modulus  $G$  of such a composite can be obtained [21]

$$G = G_m + c \frac{(G_m + \eta G_i)(G_i - G_m)}{G_i(1 + \eta)}, \quad (3)$$

where  $G_m$  is the shear modulus of the matrix,  $G_i$  is the shear modulus of the inclusion (interface),  $\eta = 0.5[1+3/(4-5\nu_i)]$ ,  $\nu_i$  is Poisson's ratio of the inclusion, and  $c$  is the volume fraction occupied by inclusions ( $c \ll 1$ ).

Equation (3) was obtained under the assumption that the matrix and the inclusions are elastic; no reservations were made about the ratio of their moduli [21]. It commonly occurs [55] that the yield stress of a crystalline material is in direct proportion to its shear modulus. Assume that the yield stress of the matrix,  $\tau_m$ , of the inclusions,  $\tau_i$ , and the effective yield stress of the composite,  $\tau_y$ , are linearly connected with the corresponding shear moduli

$$\begin{aligned} G_m &= Q_m \tau_m, \\ G_i &= Q_i \tau_i, \\ G &= Q \tau_y, \end{aligned} \quad (4)$$

where  $Q$ ,  $Q_m$  and  $Q_i$  are dimensionless factors. Additionally, assume that the values of  $\tau_m$  and  $\tau_i$  are connected with the typical structure period  $d$  corresponding to the grain size of the nanocrystalline material by the following Hall-Petch-type relationships:

$$\begin{aligned}\tau_m &= \tau_m^* + K_m d^{-k/2}, \\ \tau_i &= \tau_i^* + K_i d^{-l/2},\end{aligned}\quad (5)$$

where superscripts  $k$  and  $l$  are integers.

It can easily be shown (for example, for the cube-shaped grains) that the volume fraction of the inclusions may be estimated as  $c \approx 3\delta/d$ , if the thickness  $\delta$  is much less than the distance  $d$  between the interfaces. Then substituting (4) and (5) into (3), the following empirical dependence of the effective yield stress of the composite on the typical structure-size  $d$  is obtained [26]

$$\begin{aligned}\tau_y &= \frac{Q_m}{Q} (\tau_m^* + K_m d^{-k/2}) + \\ &3 \frac{(1-\eta)Q_m \tau_m^* + \eta Q_i \tau_i^*}{(1+\eta)Q} \delta d^{-1} + \\ &3 \frac{1-\eta}{1+\eta} \frac{Q_m}{Q} K_m \delta d^{-(1+k/2)} + \\ &3 \frac{\eta}{1+\eta} \frac{Q_i}{Q} K_i \delta d^{-(1+l/2)} - \\ &3 \frac{\delta(Q_m)^2}{(1+\eta)QQ_i} \frac{(\tau_m^*)^2 + 2\tau_m^* K_m d^{-k/2} + (K_m)^2 d^{-k}}{\tau_i^* d + K_i d^{(1-l/2)}}.\end{aligned}\quad (6)$$

The next step is to choose the values of  $k$  and  $l$ . In this case one must proceed from the specific physical mechanism that determines the yield stress in each of the phases in a particular situation. Assume that  $\tau_m$  and  $\tau_i$  are governed both by the stress in the heads of the dislocation pile-ups set against the matrix-inclusion boundary from the matrix side (Fig. 1a) and by the stress of the pile-ups in the "very intergrain" layer (Fig. 1b). The latter pile-ups provide a mechanism of intergrain sliding. The typical dimensions of pile-ups of both types are about  $d$ . This means that values of  $k = l = 1$  may be chosen to get the usual Hall-Petch law for both the matrix and the inclusion.

Now consider how the quantities  $\tau_m^*$ ,  $\tau_i^*$ ,  $K_m$  and  $K_i$  are related to each other. If the main distinction of the interfaces from the crystallites is the low atomic density of the former, it seems reasonable to assume that  $\tau_i^* \approx q\tau_m^*$  and  $K_i \approx pK_m$ , where  $q$  and  $p$  are dimensionless constants smaller than 1. Evidently, the lower the atomic density of the interface, the smaller the values of  $q$  and  $p$ .

Finally, for the sake of simplicity take  $Q \approx Q_i \approx Q_m$ . Then (6) can be easily reduced to the form [26]

$$\begin{aligned}\tau_y &= \tau_m^* + K_m d^{-1/2} - \\ &\frac{3}{1+\eta} \frac{\delta}{d} (q\tau_m^* d + pK_m d^{1/2})^{-1} \times \\ &\{[1 - q(1 - \eta + \eta q)](\tau_m^*)^2 d + \\ &[1 - p(1 - \eta + \eta p)]K_m^2 + \\ &[2 - q(1 - \eta + \eta p) - p(1 - \eta + \eta q)]\tau_m^* K_m d^{1/2}\}.\end{aligned}\quad (7)$$

Consider in greater detail the third term on the right-hand side of (7) which is accounted for by the fact that an interface is treated as an interlayer of finite thickness with its own elastic and plastic characteristics. Taking Poisson's ratio to belong to the interval 0.2-0.4 gives the following estimate for the value of  $\eta$ :  $1 \leq \eta \leq 1.25$ . For simplicity, take  $\eta \approx 1$ . Hence, the atomic density of boundaries may amount for up to 70% [56-58]. At such densities the main mechanical properties of the material (the Young's modulus, the yield stress, the fatigue stress) are known to be 4-5 times worse than the characteristics of the compact body [59]. Therefore, one can estimate  $q \approx p \approx 0.2$ .

For these values of parameters  $\eta$ ,  $q$  and  $p$  the third term in (7) turns out to be positive and is subtracted from the value of  $\tau_m$ . As expected, the low-density interlayers lower the yield stress of the composite. Using the above estimates for  $\eta$ , Eq. (7) can be expressed in its simplest form

$$\tau_y = (\tau_m^* + K_m d^{-1/2}) \left( 1 - \frac{1 - q^2}{q} \frac{3\delta}{2d} \right).\quad (8)$$

Evidently, when such a dependence is plotted in  $\tau_y \cdot d^{-1/2}$  co-ordinates, the straight line in the usual Hall-Petch law will remain straight only at large  $d$  or else as  $q \rightarrow 1$ . At  $q < 1$  its slope will gradually decrease with decreasing grain dimension down to some critical size  $d_{c1}$  where the effective Hall-Petch factor will change sign. The critical size  $d_{c1}$  can easily be found from the condition  $\partial \tau_y / \partial (d^{-1/2}) = 0$ . This equality can be reduced to the following equation

$$\begin{aligned}(d_{c1})^{-1/2} &= -\frac{\tau_m^*}{3K_m} + \\ &\frac{1}{3} \sqrt{\frac{2q}{\delta(1-q^2)}} \sqrt{1 + \frac{1-q^2}{q} \frac{(\tau_m^*)^2 \delta}{2K_m^2}}.\end{aligned}\quad (9)$$

Substituting the usual values for parameters  $\tau_m^* / K_m \approx 1 \div 100 \text{ mm}^{-1/2}$  and  $\delta \approx 1 \text{ nm}$ , the following

estimate for the critical grain size  $d_{c1}$  is obtained [26]:

$$d_{c1} \approx 9\delta \frac{1-q^2}{2q} \left( 1 - 2 \frac{\tau_m^*}{K_m} \sqrt{\frac{\delta(1-q^2)}{2q}} \right)^{-1}. \quad (10)$$

Fig. 2 presents the family of curves  $d_{c1}(q)$  calculated according to (10) at  $\delta = 1$  nm for Ti [60], Cu [32], Fe [61], Ni [24] and Ag [62]. The corresponding values of the ratio  $\tau_m^*/K_m$  are 55.46, 26.26, 8.14, 4.35 and 3.91  $\text{mm}^{-1/2}$ , respectively. The dashed line is calculated according to the approximate formula  $d_{c1} \approx 9\delta(1-q^2)/(2q)$  which may be used for estimating  $d_{c1}$  in practically any material. At  $q = 0.2$ , this expression yields the grain size  $d_{c1} \approx 22\delta = 22$  nm which corresponds to the volume fraction of boundaries  $c \approx 0.12$ .

Experimental values of  $d_{c1}$  are very spread for different materials produced by different technologies. In papers [41, 63-66], the values 8 [63], 11 [64-66], 25 [65, 66] and 45 nm [41] were reported. It is worth to note that the first value was observed in the electrodeposited nanocrystalline Ni-1.2% P alloys with very low porosity, while the others were attributed to multiphase materials produced by annealing of amorphous alloys. The authors of [41, 63] directly connected the microhardness decrease for small  $d$  with nanopores which were mainly distributed along grain boundaries and their triple junctions.

Equation (8) can be used to determine the other critical grain size,  $d_{c1}$ , at which the yield stress of a composite becomes equal to the friction stress in the matrix, i. e.,  $\tau_y = \tau_m^*$ . This critical size turns to be equal to [26]

$$d_{c2} \approx \frac{3}{2} \frac{1-q^2}{q} \delta \approx \frac{d_{c1}}{3}. \quad (11)$$

For example,  $\delta = 1$  nm and  $q \approx 0.2$  give  $d_{c1} \approx 7$  nm. Calculating the volume fraction of interface phase on the more precise, than the former, formula  $c \approx 3d\delta/(d+\delta)^2$  results in  $c \approx 0.33$  for such grain size.

Equation (8) turns out to agree pretty well with the different and apparently contradictory experimental data. For example, compare the results of the above calculations with the data from Chokshi *et al* [32] and Jang and Koch [25]. Rewriting (8) in terms of the microhardness  $H$  and substituting the values of  $H_m^*$  and  $K_m$  corresponding to coarse-grained Cu [32] and Fe [61] the families of curves,  $H(d^{1/2})$ , are obtained (see Fig. 3) for different values of  $q$ . The results given in [32] are seen to be in good agreement with the descending portion of the curve

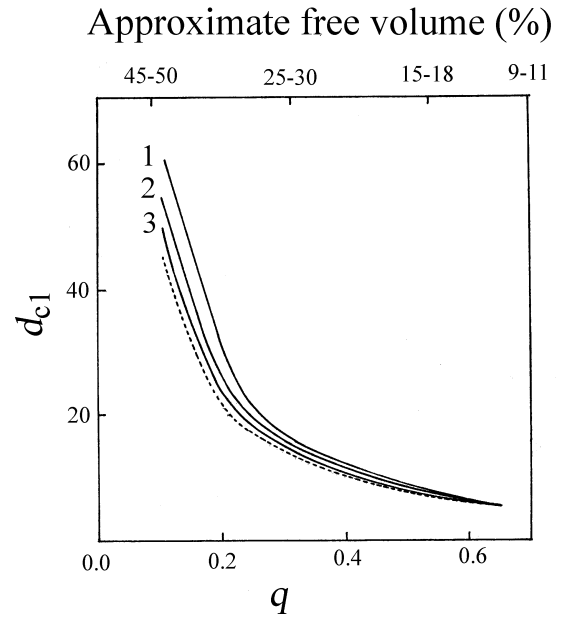


**Fig. 2.** The dependence of the critical grain size  $d_{c1}$  on the parameter  $q$  for: (1) Ti; (2) Cu; (3) Fe, Ni and Ag [26]. The dashed line is an approximate that may be applied to any material. Parameter  $q$  was put in correspondence with the atomic density of boundaries using the data from [59].

$H(d^{1/2})$ , the difference from the calculated values amounting up to 25-45% at  $q=0.2$  (Fig. 3a). A qualitatively different increasing curve  $H(d^{1/2})$  [25] fits well between the calculated curves for  $q=0.8$  and  $q=0.9$  (Fig. 3b). The difference in dependences of  $H$  on  $d^{1/2}$  obtained in [32] and [25] seems to be caused by the fact that the measurements were carried out with samples in different states of grain boundaries [26]. The measurements in [32] were performed for a nanopowder-based, as-compacted, copper sample. The boundaries of the nanocrystallite grains in the sample thus produced correspond to the surface of the as-synthesized copper particles in the pre-compaction sample. Evidently, such a procedure of producing a nanocrystalline material predetermines the low atomic density of boundaries (which increase as the internal stresses in the sample relax). The authors of [25] measured the microhardness of separate polycrystalline particles (with sizes  $\leq 1 \mu\text{m}$ ) consisting of nanocrystallites. In this case interfaces are formed from the walls of dislocation cells generated during the ball-milling process. It is clear that such a procedure produces nanocrystalline iron in which the atomic density of boundaries is significantly higher than in the former case (according to Fig. 3b it should differ from the normal value by about 5-7%).

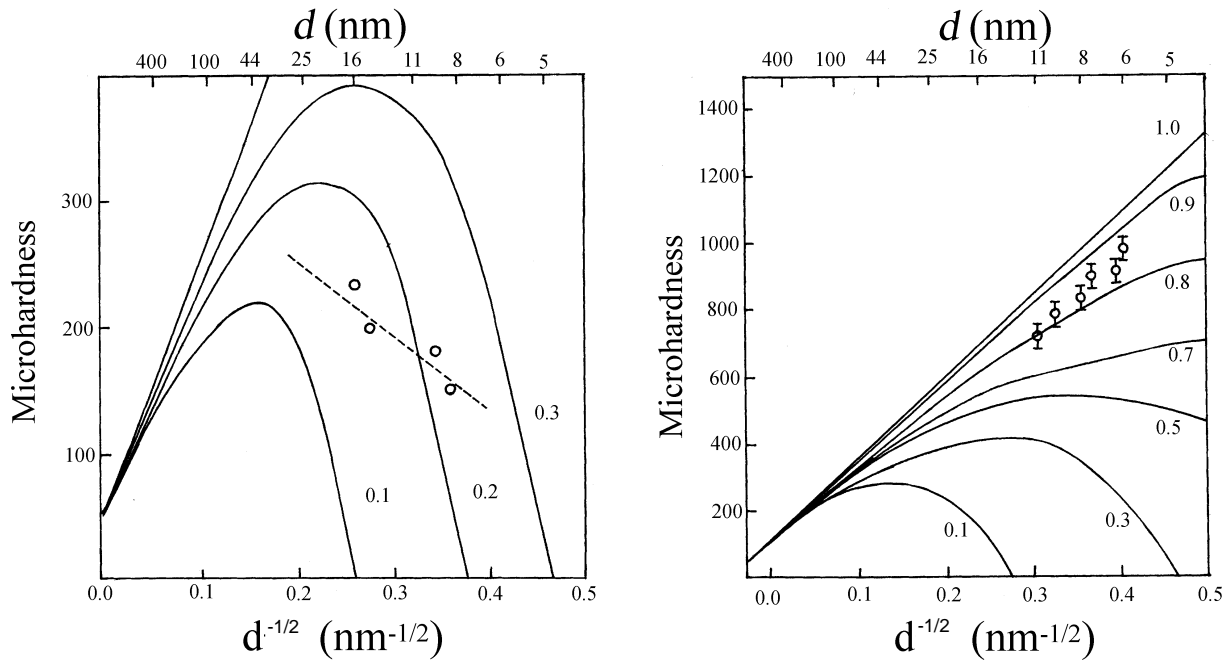


**Fig. 3.** The dependence of the microhardness on the grain size at different atomic densities of boundaries of nanocrystalline: (a) Cu, and (b) Fe [26]. This quantity is characterized by parameter  $q$ . The figures on the curves denote the values of this parameter. The straight dashed lines was drawn through the experimental points from [32] (a) and [25] (b).

Therefore, the authors of [26] showed that dependences of  $\tau_y$  and  $H$  on  $d^{-1/2}$ , for sufficiently small grains, can differ from the Hall-Petch relation but still be consistent with experimental data. The contradictions arising on comparison of experimental results obtained by different authors can be resolved in the framework of the above approach. It was concluded [26] that the type of deviation from the Hall-Petch law is determined by the atomic density of the interfaces and the range of nanocrystallite sizes under study ( $d < d_{c1}$  or  $d > d_{c1}$ ).

Similar calculations based on using the rule of mixture, were carried out in works [67-71]. The main differences were that for describing the yield stress or microhardness of the intergranular phase, they chose the data for amorphous materials of close chemical composition [67-70] and accounted for the possibility that wedge disclinations may exist in nanocrystallites [67, 68] or at the triple junctions of grain boundaries [71]. Such models were supported by the following two reasons. First, the studies of grain boundary structures in nanocrystalline materials showed by the end of eighties [48-54] that the atoms in grain boundaries are in a totally disordered state. Therefore, they assumed that the characteristics of the intergranular phase would be close enough, as a first approximation, to the properties of the corresponding amorphous material. Second,

by the same time, first metallic glass-nanosystal composites with Fe-Cr-B and TiNi alloy compositions [72-74] were synthesized at special regimes of high-pressure treatment [72,73] and rapid cooling [74]. These composites consist of nanocrystallites divided by amorphous interface, in which case the volume fractions of the nanocrystallite and amorphous phase are close. Concerning the disclination-like defects, many authors have discussed their role and behavior in structure of amorphous and nanocrystalline materials (e.g., see [75-78]) as well as in highly deformed polycrystalline metals [79]. Let us consider a model [67,68] where the simplest rule of mixture was used to estimate the yield stress of a metallic glass-nanocrystal composite with account for the influence of wedge disclinations.

Let the model composite structure be nanocrystallites which are uniformly distributed in amorphous matrix. Assume some part of the nanocrystallites contains wedge disclinations. Under the conditions of uniaxial tension, the simplest rule of mixture for the yield stress of such a composite then reads [67,68]:

$$\tau_y = f \tau_{am} + g \tau_{cr} + h \tau_d, \quad (12)$$

where  $\tau_{am}$  is the yield stress of amorphous interlayers,  $\tau_{cr}$  is the yield stress of a nanocrystallite without disclinations,  $\tau_d$  is the yield stress of a nanocrystallite with one or more disclinations, and  $f$ ,  $g$  and  $h$  are the volume fractions of the above mentioned components ( $f+g+h=1$ ).

Assume that  $\tau_{am}$  is constant and does not depend on the mean size of nanocrystallites while  $\tau_{cr}$  satisfies the Hall-Petch relationship:  $\tau_{cr} = \tau_{cr}^0 + Kd^{1/2}$ , where  $\tau_{cr}^0$  is the lattice friction and  $K$  is the Hall-Petch coefficient. The term  $\tau_d$  is determined by the following equations

$$\tau_d = \begin{cases} \tau_{cr}, & \text{if } \tau_{cr} > \tau, \\ \tau, & \text{if } \tau_{cr} < \tau. \end{cases} \quad (13)$$

Here a new parameter  $\tau$  is introduced which is the shear stress necessary for the motion of an edge dislocation intersecting an immobile wedge disclination. It is thus believed that the yield stress of a nanocrystallite with disclinations is either determined by its small size through the Hall-Petch law for  $\tau_{cr}$  or by the threshold stress  $\tau$  [80], depending on which one of them,  $\tau_{cr}$  or  $\tau$ , is higher. The latter may easily be estimated from a balance of forces acting on the dislocation after the act of its intersection with the wedge disclination. This results in  $\tau = |F|/(bd)$ , where  $b$  is the Burgers vector of the dislocation, and the force  $F$  is given by [80]

$$F(x) = -D\omega^2 b^2 \left\{ \frac{1}{2} + L \left[ \frac{2l_1 + b}{l_1(l_1 + b)} - \frac{1}{l_2} \right] - \frac{2\nu}{\omega} \ln \frac{L}{l_2} - \frac{\sqrt{l_1^2 + \omega^2 b^2}}{4l_1} - \frac{\sqrt{(l_1 + b)^2 + \omega^2 b^2}}{4(l_1 + b)} + \frac{1}{4} \ln \frac{\sqrt{l_1^2 + \omega^2 b^2} + l_1}{\sqrt{(l_1 + b)^2 + \omega^2 b^2} - l_1 - b} \right\}. \quad (14)$$

Here  $x$  denotes the distance passed by the dislocation after it has intersected the disclination,  $D = G/[2\pi(1-\nu)]$ ,  $\omega$  is the disclination power,  $2L$  the disclination length (in the given case this length is approximately equal to the nanocrystallite diameter;  $2L \approx d$ ),  $l_1 = x - \omega b$  and  $l_2 = x + b$ .

The force  $F(x)$  reaches its maximum when  $x=2b$ . In this event,  $l_1=(2-\omega)b$  and  $l_2=3b$ . Then, in examining a dislocation-disclination intersection in a nanocrystallite with diameter  $d \gg b$ , one can find  $L = d/2 \gg l_1, l_2$ . In this situation the only term in r.h.s. of (14), which is proportional to  $L$ , provides the basic contribution to the maximum force  $F(x=2b)$ . With only this contribution taken into account, the result for  $\tau$  is as follows [67,68]:

$$\tau \approx \frac{D\omega^2}{6} \frac{9 - \omega - \omega^2}{(2 - \omega)(3 - \omega)}. \quad (15)$$

Let us estimate the value of the yield stress  $\sigma_y = 2\tau_y$  for the metallic glass-nanocrystal Fe-Cr-B composite studied in [74]. Being in ignorance of appropriate numerical values for the given alloy, we used in [67,68] the data taken for a pure iron. So, the shear modulus  $G \approx 90$  GPa [81] allows to estimate  $\sigma_{am} = 2\tau_{am} \approx G/25 \approx 3.5$  GPa. The Hall-Petch parameters  $\sigma_{cr}^0 = 2\tau_{cr}^0 \approx 66$  MPa [61] and  $K = 2K \approx 26447$  MPa·nm<sup>1/2</sup> [61] lead for  $d \approx 10$  nm to  $\sigma_{cr} = 2\tau_{cr} \approx 8.3$  GPa. Substituting  $G \approx 90$  GPa,  $\nu \approx 0.3$  and  $\omega \approx \pi/6 - \pi/4$  to (15) results in  $2\tau \approx G/21 - G/8 \approx 4.3 - 11.3$  GPa. Then it follows from (13) that  $\sigma_y = 2\tau_y \approx 8.3 - 11.3$  GPa. Assuming that the nanocrystallites are packed very closely, as was in [74], one can take the volume fractions as  $f=0.4$ ,  $g=0.5$  and  $h=0.1$ . With all the above mentioned values, Eq. (12) gives:  $\sigma_y = 2\tau_y \approx 6.7$  GPa. We represent here the upper estimate of  $\sigma_y$  because the data for the real Fe-Cr-B alloy must be rather higher than those taken for a pure iron. Experiments [74] showed that metallic glass-nanocrystal composites are specified by the low plasticity, in which case their yield stress  $\sigma_y$  is close to the strength  $\sigma_b \approx 6 - 6.5$  GPa. Thus, the value obtained within the framework of the model [67,68] is close to that revealed experimentally in [74].

One can conclude that the model of metallic glass-nanocrystal composites [67,68] which allows for the presence of disclinations in a part of nanocrystallites, permits to explain unusually high mechanical properties (the microhardness, yield stress and strength) of such materials. The main reasons for significant increase of the properties with respect to those of usual homogeneous metallic glasses are high properties of nanocrystallites themselves due to their small dimensions and the role of disclinations as obstacles for dislocation motion in nanocrystallites, and very high concentration of nanocrystallites in amorphous matrix.

A very similar model which did not, however, take into account the role of disclinations, was proposed later by Carsley *et al* [69] to describe the microhardness of nanocrystalline materials. They wrote the rule of mixture (12) at  $h = 0$  in terms of microhardness as follows [69]:

$$H = \frac{(d - \delta)^3}{d^3} (H_0 + \beta d^{-1/2}) + \frac{3d^2\delta - 3d\delta^2 + \delta^3}{d^3} \left( \frac{\mu_{cr}}{12} \right), \quad (16)$$



where  $H$  is the microhardness of the nanocrystalline material as a whole,  $H_0$  and  $\beta$  are the appropriate Hall-Petch constants of a nanocrystallite, and  $\mu_{cr}$  is its shear modulus. To obtain Eq. (16), the relations  $H_0 = 3\sigma_{10}$  ( $\varepsilon = 8\%$ ) and  $\beta = 3\beta'$  ( $\varepsilon = 8\%$ ) were taken from [82] and used which connect the constants  $H_0$  and  $\beta$  with the corresponding parameters for the yield stress. As the properties of the intergranular phase were treated as those of the appropriate metallic glass, its microhardness  $H_{gb}$  was supposed to be constant and approximately equal to 1/6 the shear modulus  $\mu_{gl}$  of the metallic glass [83-85] while the latter was approximated as half that of the crystalline metal,  $\mu_{cr}/2$ .

Equation (16) was analysed in [69] with experimental values for parameters attributed to nickel [27,86], iron [87] and copper [88]. The thickness of grain boundaries was chosen as 1 nm. The  $H(d^{-1/2})$  plots demonstrate linear portions in the field  $d > 25$  nm with following deviations from the linearity for  $d < 25$  nm. Near the point  $d \approx 5$  nm, the curves achieve maximum values and decrease further at  $d < 5$  nm approaching the constant level of the microhardness calculated for the metallic glass. Comparison with the experimental data for nickel [27,86], iron [87] and copper [88] showed that the model by Carsley *et al* [69] correctly predicts the general shape of the  $H(d^{-1/2})$  curves for all three metals, and well correlates the measurements with nickel and iron. In these cases, the experimental points are close to the rising branches of the curves. For copper, however, the curve goes above the experimental points and achieves the magnitude of about 4 GPa that is 1.5-2 times higher than the maximal measured values. Moreover, the position of the maximum at the theoretical curve ( $d \approx 5$  nm) as well as the position of its dropping branch ( $d < 5$  nm) turn out to be severely shifted to the field of small grain sizes, in contrast to the experimental points [32,89] (the observations [41, 63-66] carried out later, have also testified to this misfit). It is the authors' opinion [69] that the possible reason for such a discrepancy is that they did not take into account the residual porosity of nanocrystalline copper. Let us remind that this point was treated as the key factor in the model by Gryaznov *et al* [26] in considering the differences between the  $\tau_y(d^{-1/2})$  curves for iron [25] and copper [32].

One more similar model was proposed by Kim [70]. Like in works [67-69], the properties of the intergranular phase were described as those of the metallic glass. However, in discussing the properties of nanocrystallites, Kim [70] used the conclusion by Wang *et al* [90] about the existence of a critical

nanocrystallite size  $d_c$  at which usual dislocation mechanisms of plasticity and strengthening stop to work. Accordingly, they believe that the Hall-Petch relation is true for only the case of  $d \geq d_c$ , while in smaller grains ( $d \leq d_c$ ), there is no strengthening effect and the regime of ideal plasticity is realized when the microhardness is constant and does not depend on the grain size. The numerical estimates of the critical size  $d_c$  made by Wang *et al* [90] and represented in [70], are rather spread as  $1.2 \text{ nm} < d_{c,Al} < 59.3 \text{ nm}$ ,  $1.7 \text{ nm} < d_{c,Cu} < 39.4 \text{ nm}$ ,  $1.3 \text{ nm} < d_{c,Ni} < 25.6 \text{ nm}$  and  $1.8 \text{ nm} < d_{c,Pd} < 75.3 \text{ nm}$ .

In agreement with the above assumptions, the rule of mixture for the microhardness of a nanocrystalline material was chosen as follows [70]:

$$H = \begin{cases} (H_0 + \beta d^{-1/2})f_{cr} + H_{ic}(1 - f_{cr}), & \text{if } d \geq d_c, \\ (H_0 + \beta d_c^{-1/2})f_{cr} + H_{ic}(1 - f_{cr}), & \text{if } d \leq d_c, \end{cases} \quad (17)$$

where  $H_{ic}$  is the microhardness of the intergranular phase and  $f_{cr}$  is the volume fraction of nanocrystallites. The calculations were carried out with the same three metals (Ni, Fe and Cu) as in work [69], with the same values of parameters. The critical grain sizes were taken for nickel and copper as is shown above, and the estimate 3.4 nm was chosen for iron [91]. It is rather natural that using the low limits of the ranges for  $d_c$ , Kim [70] obtained practically the same  $H(d^{-1/2})$  curves as the authors of [69] did, which have the characteristic maximums at  $d = d_{peak} \approx 3-4$  nm. The maximum condition gives [70]

$$d_{peak} = \left[ \frac{3\delta}{\beta} (H_0 - H_{ic}) + \sqrt{\left[ \frac{3\delta}{\beta} (H_0 - H_{ic}) \right]^2 + 7\delta} \right]^2, \quad (18)$$

and the numerical estimates are  $d_{peak} \approx 2.9$  nm (Cu), 3.9 nm (Ni) and 4.3 nm (Fe). Until  $d_c < d_{peak}$ , the shape of the  $H(d^{-1/2})$  curve having both the maximum point and dropping branch (for  $d < d_{peak}$ ) is conserved. However, if one takes  $d_c > d_{peak}$ , the curve shape drastically changes in the field  $d \leq d_c$  where the curve has a break (the slope decreases with a jump) at the point  $d = d_c$  and then rises monotonously with decreasing grain size. The model [70] thus predicts the two qualitatively different shapes of the  $H(d^{-1/2})$  curve depending on the value of the critical grain size. Both of them, however, demonstrate significant deviations from the usual Hall-Petch law in the field of nanoscopic grain sizes.

The theoretical  $H(d^{-1/2})$  curves of [70] are in good accordance with the experimental data for Ni [27,86] and Fe [25] as is the case with the work [69]. For copper [32,92-94], however, the experimental points of [94] are only close to the curve. All other experimental points lie much lower of the curve calculated. As the authors of [69], Kim [70] explained the reasons of the discrepancy by the necessity to account for the residual porosity of nanocrystalline materials.

Basing on the results reported in papers [67-70], one can conclude that the description of the properties of the intergranular phase through the properties of an appropriate metallic glass seems to be correct in those only cases when they consider either really metallic glass-nanocrystal composites [67,68] or the nanocrystalline materials with rather large (larger than  $\approx 20$  nm) grain sizes [69,70]. Use of this approach in models of the nanocrystalline materials with small (near or smaller than  $\approx 20$  nm) grain sizes results in over-estimating of the yield stress or microhardness and in shifting of their maximal values to the field of very small (near or smaller than  $\approx 5$  nm) grain sizes [69,70]. The authors of further works [71,95] either withdrew the idea to use the properties of metallic glass in modeling those of the intergranular phase [71] at all, or took for this not a constant value of the yield stress of metallic glass as in [67-70] but a variable quantity [95] (more precisely, it was taken constant in the region of large grain size but then sharply decreasing in proportion with decreasing grain size). Let us consider these latest results.

Konstantinidis and Aifantis [71] took the rule of mixture which is completely similar to Eq. (16) or to the first line of Eqs. (17). The only difference was the assumption that the microhardness of the intergranular phase also satisfies the Hall-Petch relation with its effective parameters  $H_{0GB}$  and  $\beta_{GB}$  (this is, in fact, the limiting case of the model by Gryaznov *et al* [26]). For simplicity, the authors [71] assumed that  $H_{0GB}=H_0$ , *i. e.*, the friction stress was supposed to be equal for both the intergranular and crystallite phases. In its turn,  $\beta_{GB}$  was estimated as the Hall-Petch  $\beta$  coefficient multiplied by a factor which would allow for the presence of obstacles for dislocation glide within grain boundaries. As the obstacles, the triple junctions of grain boundaries were considered, including those of them which contain triple line disclinations. Within the approximation of line tension for dislocations, the following estimate was obtained [71]:

$$\beta_{GB} = \beta \ln \frac{\vartheta d}{r_0} / \ln \frac{\vartheta d'_c}{r_0}, \quad (19)$$

where  $\vartheta$  is a numerical factor less than one (the ratio of the radius of curvature of a slightly curved dislocation line to the grain size),  $r_0$  is the radius of the dislocation core,  $d'_c$  is the critical grain size, such as for  $d < d'_c$ , the dislocation glide is no longer prohibited by the line tension and dislocations bypass obstacles by Orowan's mechanism. The final expression for the microhardness of a nanocrystalline material then reads [71]:

$$H = H_0 + \beta \left\{ \frac{(d - \delta)^3}{d^3} + \frac{d^3 - (d - \delta)^3}{d^3} \ln \frac{\vartheta d}{r_0} / \ln \frac{\vartheta d'_c}{r_0} \right\} d^{-1/2}. \quad (20)$$

The authors [71] carried out a detailed comparison of their  $H(d^{-1/2})$  curves corresponding to (20) with the data of many experimental measurements which were available to that time. The curves were drawn for a number of nanocrystalline materials (Cu, Fe, Pd, Ti, Ni) and intermetallics (NiP, NiZr, TiAl, Nb<sub>3</sub>Sn, FeMoSiB, FeCoSiB, FeSiB, PdCuSi). The fitting parameter  $\vartheta$  which varied from 0.0065 (for FeMoSiB) to 0.4 (for Fe), was used to fit the theoretical curves for the experimental points. In all cases, the accordance is good enough. As a result, the calculated values of the microhardness achieve their maximum at the critical grain size  $d'_c$  which vary with different materials, from 6 nm (for Fe) to 50 nm (for FeMoSiB). It was shown that the microhardness of several metals (Cu, Pd) and of all the intermetallics under investigation starts to drop with further decreasing of grain size.

Thus, significant deviations of the microhardness from the Hall-Petch law and its decrease in the region of small grain sizes is explained in [71] by peculiarities of the interaction of dislocations gliding along the grain boundaries, with the obstacles which are there. The critical grain size in the model [71] is that one at which the interaction mechanism changes from the dislocation pinning to Orowan bypassing. The maximal microhardness of a nanocrystalline material is then achieved at the critical grain size.

The rule of mixture approach has been used also in models [90, 96] of the abnormal Hall-Petch relationship in nanocrystalline materials. Wang *et al* [90] have elaborated a model describing a

nanocrystalline material as a composite with the crystallites, grain boundaries, their triple junctions and quadruple nodes playing the role of constitute phases. The model [90] led to a third order polynomial for the grain size dependence of the yield stress, which accounts for experimental data. Ovid'ko [96] has demonstrated that grain boundaries of nano-scale length are more often quasiperiodic than periodic (see also paper [97]), in which case they exhibit enhanced plastic properties. Following the model [96], quasiperiodic tilt boundaries are capable of effectively contributing to the experimentally observed abnormal Hall-Petch relationship in nanocrystalline materials.

A further and very substantial development of the rule of mixture approach was given by Kim *et al* [95]. In describing the properties of nanocrystallites, they introduced the evolution of dislocation density and the diffusion creep, while the model of diffusion flow was considered as the mechanism of grain boundary plasticity. The rule of mixture was written in the simplest form

$$\sigma = \sigma_{cr} f_{cr} + \sigma_{ic} (1 - f_{cr}), \quad (21)$$

where  $\sigma_{cr}$ ,  $\sigma_{ic}$ , and  $\sigma$  denote, respectively, the stress in nanocrystallites, in grain boundaries, and the overall stress in the nanocrystalline material. The calculation of  $\sigma_{cr}$  and  $\sigma_{ic}$  was evaluated using the assumption that the strains in both phases are the same and are equal to the macroscopic applied strain.

In a crystallite, three mechanisms of plastic deformation were considered [95] to contribute to the total deformation behavior which are: (i) the dislocation glide mechanism; (ii) the lattice diffusion mechanism in which the vacancies diffuse through the bulk of the crystallite; and (iii) the boundary diffusion mechanism in which the vacancies diffuse along the crystallite boundaries. These mechanisms were postulated to contribute to the total crystallite deformation simultaneously. For monotonic uniaxial loading, the total strain rate was assumed to be separable into elastic and plastic components. The total plastic strain rate  $\dot{\epsilon}^p$  was written as a superposition of the contributions from the individual mechanisms (i)-(iii) [95]:

$$\dot{\epsilon}^p = \dot{\epsilon}_{c,u}^p + \dot{\epsilon}_{c,b}^p + \dot{\epsilon}_{c,l}^p, \quad (22)$$

where the subscript  $c$  refers to the crystallite phase and  $u$ ,  $b$  and  $l$  stand for the deformation mechanism, *i.e.*, the dislocation glide described within a dislocation density-related unified constitutive model

[98], boundary diffusion mechanism and lattice diffusion mechanism, respectively.

The first term in (22) is determined through the following system of three equations [95,98]:

$$\dot{\epsilon}_{c,u}^p = \dot{\epsilon}_0 (\sigma / \sigma_0)^m Z^{-m/2}, \quad (23)$$

$$\frac{dZ}{d\dot{\epsilon}_{c,u}^p} = C + C_1 \sqrt{Z} - C_2 Z, \quad (24)$$

$$C_2 = C_{20} \left( \frac{\dot{\epsilon}_{c,u}^p}{\dot{\epsilon}_0} \right)^{-1/n}. \quad (25)$$

Equation (23) gives a relation between the equivalent (von Mises) plastic strain rate  $\dot{\epsilon}_{c,u}^p$  associated with the unified constitutive model of a crystallite, and the equivalent stress  $\sigma$ . Here  $Z$  is the dislocation density normalized by its initial value. The quantity  $\sigma_0$  is related to the initial dislocation density. The exponent  $m$  is stress independent for a face-centred cubic (f.c.c.) metal. The parameter  $\dot{\epsilon}_0$  is a constant normalization factor with units of strain rate. Equations (24) and (25) describe the evolution of the dislocation density with the equivalent (von Mises) plastic strain rate  $\dot{\epsilon}_{c,u}^p$ . The parameters  $C$ ,  $C_1$ ,  $C_{20}$ ,  $\sigma_0$ ,  $\dot{\epsilon}_0$  and  $\dot{\epsilon}_0$  were considered constant for f.c.c. metals at low temperatures. The exponents  $m$  and  $n$  are inversely proportional to the absolute temperature  $T$  and were also considered constant for a given temperature  $T$ .

The plastic strain rate of a crystallite associated with the lattice diffusion mechanism (Nabarro-Herring creep) is given by

$$\dot{\epsilon}_{c,l}^p = 14 \frac{\Omega \sigma}{kT} \frac{D_{ld,0}^{sd}}{d^2} \exp\left(-\frac{Q_{ld}}{kT}\right), \quad (26)$$

and that associated with the grain-boundary diffusion mechanism (Coble creep) by

$$\dot{\epsilon}_{c,b}^p = 14\pi \frac{\Omega \sigma}{kT} \frac{\delta D_{bd,0}^{sd}}{d^3} \exp\left(-\frac{Q_{bd}}{kT}\right). \quad (27)$$

Here  $k$  is the Boltzmann constant,  $\Omega$  is the atomic volume,  $Q_{ld}$  is the activation energy for lattice self-diffusion, and  $Q_{bd}$  is the activation energy for boundary self-diffusion. The pre-exponential factors  $D_{ld,0}^{sd}$  and  $D_{bd,0}^{sd}$  refer to the lattice diffusion and grain-boundary diffusion, respectively.

It is worth noting that in [95] (as before in [70]), a critical grain size  $d_c$  ( $\approx 8.2$  nm for Cu [90]) was introduced such as the dislocation glide mechanism of plastic deformation works in large enough nano-

crystallites with  $d > d_c$ . In smaller nanocrystallites, only the diffusion mechanisms were considered to be active.

In describing the deformation behavior of the intergranular phase, the authors [95] believed that the plastic deformation is associated with diffusional mass transport along the boundaries at small grain sizes, while at large grain sizes, the grain-boundary interlayers behave like a metallic glass under the homogeneous deformation. Accordingly, the strength of the intergranular phase was assumed to increase up to an upper limit and then to stay at that level as the grain size increases. This upper limit was set to be the strength of the material in the amorphous state. The minimal grain size which corresponds to this upper limit as well as the values of the yield stress are determined by the strain rate of the intergranular phase [95],

$$\dot{\epsilon}_{bd} = \frac{\Omega_b \sigma (2d - \delta) D_{bd}^{sd}}{kT d^3}, \quad (28)$$

where  $\Omega_b$  is the atomic volume in the grain boundary,  $\sigma$  is the component of the local stress normal to the boundary, and  $D_{bd}^{sd}$  is the coefficient of self-diffusion within the grain boundary.

It was specially noted [95] that in the model under consideration, the same grain boundaries were regarded as "channels" for material flow of two phase: the boundary phase itself and the crystallite. In other words, two separate flows co-exist in one such "channel". One of the flows provides the boundary diffusion in crystallites and the Coble creep mechanism while the other flow is responsible for the plastic deformation of the grain boundaries.

The model of [95] was analysed with the data for nanocrystalline copper. The yield stress was determined for the crystallite phase by substituting (22) with (23)-(27) to the usual governing equation of the theory of plasticity, and for the intergranular phase from the expression (28). The overall yield stress of the nanocrystalline material was calculated with the rule of mixture (21). The stress-strain curves and the 0.2 % offset stress  $\sigma_{0.2}$  for the crystallite phase were studied in wide ranges of grain sizes (from 10 nm to 1000 nm) and of strain rates (from  $10^{-5} \text{ s}^{-1}$  to  $10^{-3} \text{ s}^{-1}$ ). As the grain size diminished, the stress  $\sigma_{0.2}$  firstly increased, achieved its maximal value and then decreased. The deviations of the  $\sigma_{0.2}(d^{-1/2})$  curve from the usual linear Hall-Petch law began as earlier as the strain rate was smaller. Accordingly, the maximal value of the stress  $\sigma_{0.2}$  was smaller and achieved earlier (from  $\approx 300 \text{ MPa}$  at  $d \approx 100 \text{ nm}$  and  $\dot{\epsilon} = 10^{-5} \text{ s}^{-1}$  to  $\approx 600 \text{ MPa}$  at  $d \approx 20 \text{ nm}$  and  $\dot{\epsilon} = 10^{-3} \text{ s}^{-1}$ ).

The investigation of the relative contributions of different mechanisms (the dislocation glide, the boundary and lattice diffusion) to the strain rate of nanocrystallites showed that the contribution of the lattice diffusion may be neglected in any practical case. At small grain sizes, the boundary diffusion is a dominant deformation mechanism, while in coarse grains, the strain rate for the dislocation glide mechanism dominates completely. The relative contributions of the dislocation glide and the boundary diffusion mechanisms become equal at approximately 16 nm (for  $\dot{\epsilon} = 10^{-3} \text{ s}^{-1}$ ) and 55 nm (for  $\dot{\epsilon} = 10^{-5} \text{ s}^{-1}$ ). In accordance to this analysis, the  $\sigma(\epsilon)$  curves demonstrated usual deformation strengthening of crystallites with sizes of 100 nm and 1000 nm, where the contribution of the dislocation glide mechanism still dominates, and the complete absence of the strengthening in nanocrystallites with sizes of 10 nm, where the Coble creep by the boundary diffusion prevails.

A comparison of the overall  $\sigma(\epsilon)$  and  $\sigma_{0.2}(d^{-1/2})$  curves [95] with the results of experiments [20, 34, 94, 99, 100] carried out with samples of poly- and nanocrystalline copper having low porosity showed, in general, a good agreement, although the model [95] gives sometimes quite overestimated or underestimated values. A great achievement is that the maximums at the  $\sigma_{0.2}(d^{-1/2})$  curves have shifted to the range of coarser grains (now from  $\approx 16 \text{ nm}$  at  $\dot{\epsilon} = 10^{-3} \text{ s}^{-1}$  to  $\approx 70 \text{ nm}$  at  $\dot{\epsilon} = 10^{-5} \text{ s}^{-1}$ ) in contrast to the previous models [69,70] (they had given the values near or smaller than 5 nm) that is a natural corollary of the refusal to consider the intergranular phase as an amorphous material, in the range of small grain sizes. The remaining discrepancies between the predictions of the model and the experimental data were referred by the authors [95] to the experimental uncertainties as well as to the necessity to take into account the influence of the residual porosity of nanocrystalline materials. Note that the last reason was already mentioned in earlier works [69,70].

The authors [95] thus made an essential step ahead in modeling the plastic deformation of nanocrystalline materials within the rule-of-mixture approach. Allowing different possible mechanisms of crystallite plasticity and withdrawing the representation of grain boundaries through the interlayers of an amorphous material with a constantly high value of strength, they obtained quite realistic curves  $\sigma(\epsilon)$  and  $\sigma_{0.2}(d^{-1/2})$  in a wide range of strain rates. It is natural that such a refined model had to be restricted in some other respects (only uniaxial loading, only f.c.c. metals, only low porosity). However, the au-

thors [95] claimed that a new quantitative model was in progress which would incorporate the effects of porosity and of grain size distribution.

Concluding the discussion of the afore mentioned models which were aimed to obtain, within the rule-of-mixture approach, the Hall-Petch-type dependences for nanocrystalline materials and to study the reasons and peculiarities of the deviations from the classical linear law,  $\sigma_y(d^{-1/2}) \sim d^{-1/2}$ , one can state the following inferences.

- The rule-of-mixture approach is a simple and effective way to obtain and study the Hall-Petch-type relation for nanocrystalline materials.
- The rule of mixture may be used in a general empirical form without dwelling on the particular physical mechanisms of plastic deformation of crystallites and grain boundaries, as well as it may account for different mechanisms of motion and interaction of defects in both (crystallite and intergranular) the phases.
- The models of the intergranular phase which are based on a similarity with the interlayers of an amorphous material having a constantly high value of strength, seem to be applicable to only the real metallic glass-nanocrystal composites and to be inapplicable to usual nanocrystalline materials where these models lead to essential disagreements with experimental data in the range of small grain sizes.
- One of the key problems in describing the Hall-Petch-type relation for real nanocrystalline materials is the account for the residual porosity of samples.

### 3. PHYSICAL MECHANISMS OF PLASTIC DEFORMATION IN NANOCRYSTALLINE MATERIALS

In this section we will consider theoretical models focusing on physical mechanisms of plastic flow in nanocrystalline materials. In doing so, first, we will discuss models based on the idea on the conventional lattice dislocation motion in nanograin interiors as the dominant deformation mechanism in nanocrystalline materials (see subsection 3.1). Then, the deformation mechanisms associated with the active role of grain boundaries in nanocrystalline materials will be considered (see subsection 3.2). Finally, we will analyse the combined effects of the competition between various deformation mechanisms (depending on the grain size) and a distribution of grain size on the deformation behavior of nanocrystalline materials (see subsection 3.3).

#### 3.1. Lattice dislocation motion in nanocrystalline materials

There are models that treat motion of lattice dislocations in grain interiors to be the dominant deformation mechanism in nanocrystalline materials, as with coarse-grained polycrystals. In the framework of this approach, the experimentally documented deviations from the conventional Hall-Petch relationship in nanocrystalline materials are explained as those related to the influence of the grain size reduction and high-density ensembles of grain boundaries on the formation of lattice dislocation pile-ups in grain interiors and the penetration of lattice dislocations through grain boundaries in such materials.

Let us start analysis of this approach with a brief discussion of models describing the classical Hall-Petch relationship (1) in coarse-grained polycrystals. Most of these models can be rationalized in terms of a dislocation pile-up model. These are reviewed in detail by Li and Chou [101]. In deriving Hall-Petch relation, the role of grain boundaries as a barrier to dislocation motion is considered in various models. In one type of models [102-104], grain boundary acts as a barrier to pile-up of dislocations, causing stresses to concentrate and activating dislocation sources in the neighboring grains, thus initiating slip from grain to grain. In the other type of models [19, 105, 106], the grain boundaries are regarded as dislocations barriers limiting the mean free path of the dislocations, thereby increasing strain hardening, resulting in a Hall-Petch type relation. A review of the various competing theories of strengthening by grain refinement has been discussed by several workers. (For a more recent survey, see Lasalmonie and Strudel [24].) It is clear that a variety of processes, both dislocation and non-dislocation based, could be postulated. It is possible that several of these processes could compete or reinforce the deformation process.

Now let us turn to a discussion of models focusing on lattice dislocation mechanism of plastic flow in nanocrystalline materials. First, let us consider dislocation model of Pande and Masumura [107]. The assumption made in this model is that the classical Hall-Petch dislocation pile-up model is still dominant with the sole exception that the analysis must take into account of the fact that in the nanometer size grains, the number of dislocations within a grain cannot be very large. Further at still smaller grain sizes, this mechanism should cease when there are only two dislocations in the pile-up.

Pande and Masumura [107] by considering the conventional Hall-Petch model showed that a dislocation theory for the Hall-Petch effect gives a linear dependence of  $\tau$  on  $d^{-1/2}$  only when there are large number of dislocations in a pile-up and plasticity is not source limited. In this regime, the yield stress increases as  $d$  decreases because the pile-ups contain fewer dislocations, the stress concentration at the head falls and a larger applied stress is required to compensate. When the number of dislocations falls to one, no further increase in the yield stress is possible and it saturates. If, however, sources must operate in each grain, an additional component of the yield stress exists of at least  $Gb/d$  and the yield stress should rise as  $d^{-1}$ . Thus from these arguments, at a small grain size, either the yield stress should rise faster than  $d^{-1/2}$  or it should saturate, but it should not decrease. If the number of dislocations  $n$  in a pile-up is not too large the length of the pile-up  $L$  is not linear in  $n$  but an additional term is necessary. Chou [108] gives the relation

$$L \cong \frac{A}{2\tau} \left[ 4 \left( n + m - 1 - 2i_1 \left( \frac{2n}{3} \right)^{1/3} \right) \right], \quad (29)$$

where  $i_1/6^{1/3} = 1.85575$ . Pande and Masumura [107] give an improved expression *viz.*,

$$L \cong \frac{A}{2\tau} \left[ 2(n + m - 1)^{1/2} - \frac{i_1 + \varepsilon}{12^{1/3} (n + m - 1)^{1/6}} i_1 \right], \quad (30)$$

where  $\varepsilon$  is a small correction term ( $\varepsilon \ll 1$ ) and can be neglected. They find that for small grain sizes there are additional terms to Hall-Petch relation *viz.*,

$$s = \lambda^{-1/2} + c_1 (\lambda^{-1/2})^{5/3} + c_2 (\lambda^{-1/2})^{7/3}, \quad (31)$$

where  $s = \tau/[m\tau^*]$ ,  $c_1 = -0.6881$ ,  $c_2 = 0.21339$  and  $l = Lm\tau^*/2A$ . This model recovers classical Hall-Petch at large grain sizes but for smaller grain sizes the  $\tau$  levels off. This model therefore cannot explain a drop in  $\tau$ .

**Other Dislocation Mechanisms.** Valiev *et al* [109] mention a creep mechanism in which dislocations require a specific amount of time to be absorbed into the grain boundary. Such times involve a characteristic length of 30 nm that is approximately the distance at which the image of the dislocation “disappears.” But detailed mechanism relating  $\tau$  with  $d$  in this region is not available.

In a recent publication, Malygin [110] seems to have provided just such a theory based on a dislocation mechanism. The dislocation density  $\rho(d)$  at

any grain size,  $d$ , is related in the usual fashion to the square of yield stress and an expression is obtained that connects  $\rho$  to the grain size. The expression is based on the assumption that grain boundaries act predominately as sinks for dislocations (just the opposite to that used by Li [111], who postulated that grain boundaries could be sources for dislocation generation). In Malygin’s model, as the grains become finer and finer, more and more dislocations are absorbed by the grain boundaries leading ultimately to a drop in dislocation density and hence in the flow stress since the two are directly related as mentioned above. The model is attractive, and should be considered further. At present, we merely point out two problems with the model. First, it is doubtful if the dislocations play the same role whether the grains are large or small. It is more likely that dislocations in ultrafine grains if present at all, are confined to grain boundaries [112]. Second, in Malygin’s model [110], the stress calculated is a work-hardened flow stress rather than a yield stress.

Lu and Sui [113] assume that both the energy and free volume of grain boundaries decrease with reduction of the grain size  $d$ . This gives rise to enhancement of lattice dislocation penetration through grain boundaries and the corresponding softening of nanocrystalline materials. Following Seattergood and Koch [114], the yield stress of fine-grained materials is controlled by intersection of mobile lattice dislocations with dislocation networks at grain boundaries. In this context, with the dislocation line tension assumed to be size dependent, there is some critical grain size that corresponds to a transition from cutting to Orowan bypassing of the dislocation network. This critical grain size characterizes the experimentally detected transition from the conventional to inverse Hall-Petch relationship with reducing the grain size  $d$ . Nazarov *et al* [115], Nazarov [116] and Lian *et al* [117] have developed models similar to that of Pande and Masumura [107], focusing on the influence of the grain size  $d$  on the parameters of lattice dislocation pile-ups in grain interiors.

Zaichenko and Glezer [118] have described the role of grain boundary disclinations - rotational defects formed at triple junctions - as sinks and sources of lattice dislocations moving in grain interiors and causing plastic flow in nanocrystalline materials. Following the model of Zaichenko and Glezer [118], lattice dislocations are emitted and absorbed at opposite triple junctions of grain boundaries, containing disclinations (formed during fabrication of nanocrystalline materials). In doing so, the

yield stress is caused by interaction between grain boundary disclinations and lattice dislocations moving in grain interiors. The disclinations move in vicinities of their initial positions (corresponding to non-deformed state of a material) at grain boundary junctions when they emit and absorb lattice dislocations.

Despite of the good correspondences between theoretically predicted  $\tau(d)$  dependences and experimental data, all the above models based on the representations on the lattice dislocation mechanism of plastic flow in nanocrystalline materials meet the question if lattice dislocations exist and play the same role in nanograin interiors as with conventional coarse grains. As pointed out in papers [119-121], the existence of dislocations in either free nanoparticles or nanograins composing a nanocrystalline aggregate is energetically unfavourable, if their characteristic size, nanoparticle diameter or grain size, is lower than some critical size which depends on such material characteristics as the shear modulus and the resistance to dislocation motion. The dislocation instability in nanovolumes is related to the effect of the so-called image forces occurring due to the elastic interaction between dislocations and either free surface of nanoparticle or grain boundaries adjacent to a nanograin [119-121]. The paucity of mobile dislocations in nanograins has been well documented in electron microscopy experiments [11, 122].

### 3.2. Evolution of defects and grain boundary structures in plastically deformed nanocrystalline materials

Let us discuss theoretical models describing plastic flow in nanocrystalline materials as that occurring mostly via deformation mechanisms associated with the active role of grain boundaries. Such deformation mechanisms are, in particular, grain boundary sliding and diffusion plasticity mechanisms related to grain boundary diffusion.

Hahn *et al* [123] treat the grain boundary sliding as the deformation mechanism effectively competing with the conventional lattice dislocation motion in nanocrystalline materials. In doing so, the grain boundary sliding occurs via motion of mobile grain boundary dislocations with Burgers vectors parallel with boundary planes. Triple junctions of grain boundaries, where boundary planes with various orientations join together, serve as obstacles for grain boundary dislocation motion. In order to overcome the obstacles, grain boundary structures un-

dergo the grain-boundary-sliding accommodation transformations; the same comes into play in superplastic deformation characterized by the dominant grain boundary sliding. The model of Hahn *et al* [123] describes local migration of grain boundaries as the accommodation mechanism for the grain boundary sliding. More precisely, local migration of grain boundaries is considered to provide the formation of tentatively planar ensemble of grain boundaries along which intensive plastic shear via correlated grain boundary sliding processes occurs. These macroscopic planar grain boundary structures are associated with shear bands where high (super)plastic deformation is localized, resulting in a large macroscopic deformation of a nanocrystalline sample.

The local migration of grain boundaries occurs more effectively than other diffusion accommodation mechanisms, because characteristic spatial scale of diffusion associated with the local migration of grain boundaries is very small; it is in the order of the grain boundary thickness. In these circumstances, the strain-rate controlling process is the grain boundary sliding. Though there is experimental evidence for local migration of grain boundaries in superplastically deformed polycrystals [124], at present, there are no direct experimental data confirming the model of Hahn *et al* [123] in the case of nanocrystalline materials. Also, this model does not quantitatively describe the yield dependence on the grain size.

Results of computer simulations have been reported [125, 126] on plastic deformation in model f.c.c. metals. Thus, the competition between lattice dislocation motion and grain boundary sliding has been revealed. For small grain size (tentatively  $< 10$  nm) all deformation is accommodated in grain boundaries. At higher grain sizes, the intergrain deformation is observed which occurs via motion of partial dislocations in grain interiors, in which case these dislocations are emitted and absorbed in opposite grain boundaries. Thus, results of computer modeling [125, 126] indicate in favor of the competition between conventional intergrain sliding via lattice dislocation motion and grain boundary sliding in nanocrystalline materials. The role of grain boundary sliding increases with reducing the grain size.

Song *et al* [13] have distinguished the two branches of the grain size dependence of the yield stress. One branch is realized at large grain sizes ( $d > d_{cr}$ ), which is described by the classical Hall-Petch relationship (1). At small grain sizes ( $d < d_{cr}$ ), following the model of Song *et al* [13], a nanocrystalline material behaves as a coherent-pre-

precipitate strengthened two-phase alloy in which the grain boundary phase plays the role of matrix, and each of the grains embeds into the matrix coherently. In this region, the yield stress is given as:

$$\tau = \tilde{\tau} + \frac{\gamma_0}{\tilde{b}} f_{cr}, \quad (32)$$

where  $\tilde{\tau}$  denotes the yield stress of the matrix (grain boundary phase) without obstacles (grains),  $\gamma_0$  the interphase boundary energy,  $\tilde{b}$  the Burgers vector magnitude that characterizes grain boundary dislocations as carriers of plastic flow in the matrix, and  $f_{cr}$  the volume fraction of crystalline grains (playing the role of obstacles for grain boundary dislocations), which can be approximately written as follows:

$$f_{cr} = \left( \frac{d - \Delta}{d} \right)^3. \quad (33)$$

Here  $\Delta$  is the effective grain boundary thickness, and  $d$  is the mean grain size. Formulae (32) and (33) account for experimental data on the abnormal Hall-Petch relationship at some values of model parameters. However, use of formula (32) which initially describes strengthening of coherent-precipitate two-phase alloys is questionable in the case of nanocrystalline materials, because it is based on the assumptions that carriers of plastic flow in the matrix (grain boundaries) and coherently embedded second-phase particles (grains) are the same. This assumption is very discussive. Crystalline nano-grains and grain boundary structures are essentially different, contain dislocations with essentially different characteristics and can not be matched coherently.

The model of Ovid'ko [127] describes the grain boundary sliding as the dominant deformation mechanism of plastic flow in nanocrystalline materials at elementary, nano-scale and meso-scale levels (Fig. 4). Carriers of plastic deformation at the elementary length scale are treated to be conventional defects of crystal and grain-boundary structures, that is, crystal-lattice dislocations and grain-boundary dislocations with Burgers vectors and defect core sizes being in the order of the crystal lattice parameter (Fig. 4a). In order to describe plastic deformation at the nano-scale level, the paper [127] introduces the notion of nano-dislocations with variable Burgers vectors. Each nano-dislocation is defined as a superposition of sliding grain boundary dislocations belonging to one grain boundary (Fig. 4b). In other words, a nano-dislocation is a kind of a superdislocation which consists of all mobile grain

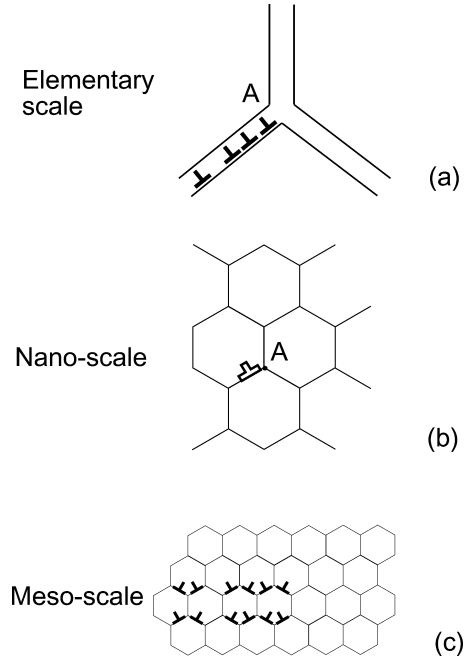


**Fig. 4.** Carriers of plastic flow in nanocrystalline materials at various length scales: (a) elemental grain boundary dislocations at atomistic length scale; (b) nano-dislocation (group of elemental dislocations) at nano-scale; (c) group of nano-dislocations (shear band) at meso-scale.

boundary dislocations at one nano-scale grain boundary. Mobile grain boundary dislocations belonging to one boundary exhibit a correlated behavior in response to applied shear stress due to the strong elastic interaction between them and their low-barrier motion between grain boundary junctions. This allows one to effectively describe their correlated motion under the shear stress action as the motion of a nano-dislocation. The motion of a nano-dislocation is accompanied by various structural transformations including various grain-boundary sliding accommodation processes, in which case elementary dislocations composing the nano-dislocation move and undergo transformations accompanied by changes of their sum density and spatial arrangement. Such changes are effectively described as evolution of Burgers vector of the moving nano-dislocation during its motion (Fig. 5). Thus, as with dislocation having variable Burgers vectors in amorphous solids [128-130], nano-dislocations with variable Burgers vectors serve as carriers of plastic flow at the nano-scale level in nanocrystalline materials [127].

In general, plastic deformation in nanocrystalline materials can be spatially homogeneous or inhomogeneous being localized in narrow shear



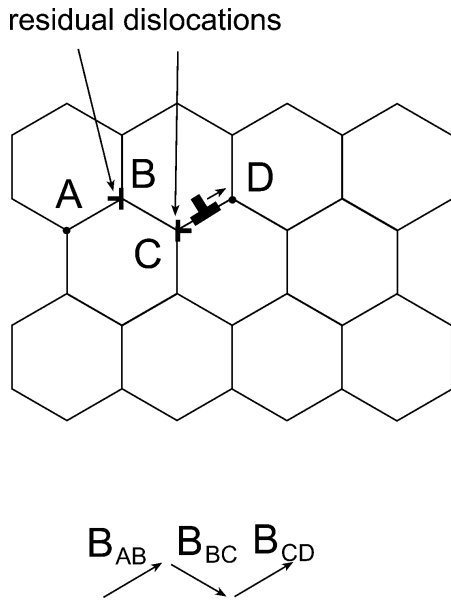


**Fig. 5.** Nano-dislocation moves along grain boundaries whose planes are close to the plane of the maximum shear stress. Its Burgers vector evolves in accordance with orientations of grain boundary planes. Residual dislocations are formed behind the moving nano-dislocation.

bands; see, e.g., experimental data [131,132]. In the latter case, development of a shear band can be effectively described as propagation of a group of nano-dislocations through the section of the deformed nanocrystalline film (Fig. 4c) [127].

Let us consider the model of Chokshi *et al* [32]. Clearly, at sufficiently small grain sizes, the Hall-Petch model based upon lattice dislocations may not be operative. In this region, Chokshi *et al* [32] have proposed room temperature Coble creep as the mechanism to explain their results. Certainly, there is an order of magnitude agreement and the trend is correct, however, the functional dependence of  $\tau$  on  $d$  is incorrect as pointed out by Neih and Wadsworth [91]. Conventional Coble creep demands that  $\tau \sim d^3 \propto [d^{-1/2}]^6$ , i.e., the  $\tau$  vs.  $d^{-1/2}$  curve falls very steeply as  $d^{-1/2}$  increases. This is not found experimentally [32]. When we fit the data of Chokshi *et al* to a Coble type equation, viz.,

$$\tau = \gamma + \alpha d^3, \quad (34)$$

we find that the fit requires a large value of  $\gamma = 360$  MPa which suggests that the threshold stress for Coble creep is of the form  $Gb/d$  [133] since this would have the correct magnitude for a 10 nm grain size. The origin of this threshold is related to vacan-

cies that are created and destroyed on dislocations climbing along grain boundaries. The dislocations are pinned at grain boundaries nodes and require a stress of  $Gb/d$  to climb. Chokshi *et al* [32] showed that their data, however, fit better the relation

$$\tau = \beta - K' d^{-1/2}, \quad (35)$$

with  $\beta = 937$  MPa and  $K' = 0.027$  MPa m<sup>1/2</sup> instead of Eq. (34). Eq. (35) cannot be related simply to any known mechanism.

Even if the Coble creep argument were valid for grain sizes  $d < 30$  nm, we still have to explain the behavior in the 20 to 200 nm range. This is evidently the transition regime between the Hall-Petch and Coble creep-like behavior. The transition regime is effectively described with a distribution of grain size taken into account. It is the subject of next section.

### 3.3. Competition between deformation mechanisms and effect of a distribution of grain size in plastically deformed nanocrystalline materials

From the previous discussion, it is quite obvious that a unified model of grain size strengthening applicable to a wide range of grain size was lacking. Masumura *et al* [18] provided such a model and developed an analytical expression for  $\tau$  as a function of the inverse square root of  $d$  in a simple and approximate manner that could be compared with experimental data over a wide range of grain sizes. This model is summarized below. The assumptions in this model are:

1. It is assumed that polycrystals with a relatively large average grain size obey the classical Hall-Petch relation (The departure from the linear Hall-Petch relation in pile-up model has been discussed and is ignored in the first approximation but can be incorporated easily (see subsection Dislocation Model of Pande and Masumura in section 3.1)).
2. At the other extreme for very small grain sizes, it is assumed that Coble creep is active and that the  $\tau$  vs  $d$  relationship is given by

$$\tau_c = A/d + Bd^3, \quad (36)$$

where  $B$  is both temperature and strain-rate dependent. The additional term  $A/d$  (the threshold term) can be large if  $d$  is in the nanometer range. For intermediate grain sizes, both mechanisms might be active if the specimen has range of grain

size distribution. A threshold of the  $A/d$  has been proposed by others (Sastry [134]).

3. The statistical nature of the grain sizes in a polycrystal is taken into consideration by using an analysis similar to Kurzydowski [135]. The volume of the grains are assumed to be log-normally distributed

$$f(v) = \frac{1}{v\sqrt{2\pi}s_{\ln v}} \exp\left[-\frac{(\ln v - m_{\ln v})^2}{s_{\ln v}^2}\right], \quad (37)$$

where  $m_{\ln v}$  and  $s_{\ln v}$  are the mean value and standard deviation of  $\ln v$ , respectively, and where the  $m_v$  is the mean volume of all the grains,

$$m_v = \int_0^{\infty} v f(v) dv = \exp[m_{\ln v} + (s_{\ln v})^2], \quad (38)$$

and can also be written as  $m_v = \kappa \bar{d}^3$  where  $\bar{d}$  is mean grain size and with  $\kappa$  being a geometrical shape factor considered for this analysis to be equal to 1.

4. Finally, it is assumed that a grain size  $d^*$  exists at which value the classical Hall-Petch mechanism switches to the Coble creep mechanism,  $\tau_{hp} = \tau_c$  at  $d = d^*$ . Using Eqs. (1) and (36), we have

$$k(d^*)^{-1/2} = A/d^* + B(d^*)^3 \quad (39)$$

from which  $d^*$  can be determined.

Then the yield stress after averaging is given as

$$\langle \tau - \tau_0 \rangle = F_{hp} + F_c, \quad (40)$$

where

$$F_{hp} = \frac{1}{m_v} \int_v \tau_{hp} dv, \quad (41)$$

and

$$F_c = \frac{1}{m_v} \int_v \tau_c dv. \quad (42)$$

We define

$$\xi = \frac{d}{d^*} \quad \text{and} \quad \sigma = s_{\ln v} \quad (43)$$

along with

$$\Lambda(\xi; \sigma, \alpha) = \xi^{3\alpha} \exp\left[\frac{\sigma^2}{2} \alpha(\alpha + 1)\right] \quad (44)$$

and

$$\Phi(v; \sigma, \alpha) = \text{erf}\left\{\left(\frac{1}{2\sigma^2}\right)^{1/2} \left(\ln\left[\frac{v}{m_v}\right] - \frac{\sigma^2}{2}(2\alpha^2 + 1)\right)\right\}, \quad (45)$$

where  $\text{erf}\{\}$  is the error function. Further defining additional normalized variables,

$$F_{c1} = \Lambda(2d^*)^{-1} f_{c1}; \quad (46)$$

$$f_{c1} = \Lambda(\xi; \sigma, -1/3)[\Phi(\xi; \sigma, -1/3) + 1]$$

and

$$F_{c2} = B \frac{(d^*)^3}{2} f_{c2}; \quad (47)$$

$$f_{c2} = \Lambda(\xi; \sigma, 1)[\Phi(\xi; \sigma, 1) + 1]$$

and

$$p = \frac{A/d}{B(d^*)^3}, \quad (48)$$

we have a normalized form of the yield stress,  $\tau_n$ , as a function of the scaled grain size  $\xi$ , grain size parameter  $\sigma$  and  $p$ ,

$$\tau_n = \frac{2}{k(d^*)^{-1/2}} \langle \tau - \tau_0 \rangle = f_{hp} \frac{pf_{c1} + f_{c2}}{1 + p}. \quad (49)$$

The parameter  $p$  is the ratio of Coble threshold stress to conventional stress evaluated at  $d^*$  where the transition from Coble creep to Hall-Petch strengthening occurs. For each  $p$  and  $\sigma$  universal curve is obtained with the form and shape of the curve similar to experimental data. Eq. (49) is the key result of their analysis. In Fig. 6 the yield stress of NiP data of McMahon and Erb [136], after normalization, is compared with this equation. The threshold stress as compared to the Coble creep stress is small in this material. The value for  $d^* = 5.5$  nm as determined from this analysis is in agreement with the original hardness data where the hardness (or stress) begins to decrease with decreasing grain size at a grain size of 5-6 nm.

Thus this model uses conventional Hall-Petch strengthening for larger grains and Coble creep with a threshold stress for smaller grains. In a material with a distribution of grain sizes, a fraction of grains deforms by a dislocation glide process and the rest

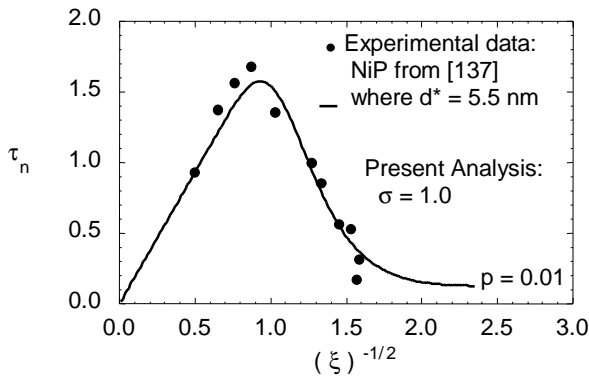


**Fig. 6.** Plot of normalized stress,  $\tau_n$ , as a function of the reduced variable  $\xi^{-1/2}$ .

by vacancy transport. As the average grain size decreases, the fraction deforming by glide decreases and the overall response changes from strengthening to softening. The exact form of the yield stress against grain size curve depends on the relative values of Hall-Petch slope  $k$ , the conventional Coble constant  $B$ , the threshold constant  $A$  and the width of the grain size distribution  $\beta$ .

**Refinement to the model of Masumura, Hazzledine and Pande.** It should be noted that the model of Masumura *et al* [18] only takes into account the first term of Eq. (31) in their calculations. Additional terms however can easily be taken into consideration and the final result will include two more terms involving error functions. Preliminary estimate indicates that this will not substantially change their result but will make the transition from rising  $\tau$  to decreasing  $\tau$  more gradual.

Thus, following model of Masumura *et al* [18], both dislocations and Coble creep play a significant role leading to a fuller understanding of Hall-Petch type relation over the whole range of grain sizes. Further it is unrealistic to expect that unlimited strength is available simply by reducing the grain size, though in some materials, considerable strengthening can be achieved by nanocrystalline processing. Further strengthening in principle is possible, if somehow Coble creep could be reduced.

#### 4. CONCLUDING REMARKS

Thus in this paper we have reviewed theoretical models of plastic flow in nanocrystalline materials with the special attention paid to the abnormal Hall-Petch effect, that is, the softening of a nanocrystalline material with reducing the mean grain size  $d$ . In general, there are the two key theo-

retical approaches to a description of the abnormal Hall-Petch effect which is inherent to nanocrystalline materials in contrast to conventional coarse-grained polycrystals where the yield stress, according to the classical Hall-Petch relationship (1), grows with reduction of the grain size  $d$ . The first approach treats nanocrystalline materials as composites with grain boundaries and grain interiors playing the role of constituent phases. In the framework of this approach, the yield stress is given by the so-called rule of mixture (conventionally used in the theory of composites) as some weighted sum of the yield stresses that characterize the grain boundary phase and grain interiors. The second approach focuses on microscopic (physical) mechanisms of plastic deformation in nanocrystalline materials. This approach attributes the abnormal Hall-Petch effect to either essential modification of conventional lattice dislocation motion or transition to another deformation mechanism (associated with the active role of grain boundaries) in plastically deformed nanocrystalline materials due to nano-scale effects and the existence of high-density ensembles of grain boundaries.

Different theoretical models give different explanations of the abnormal Hall-Petch relationship, in which case most of them well account for the corresponding experimental data. However, it is extremely difficult to experimentally identify the deformation mechanism(s) in nanocrystalline materials due to their very complicated nano-scale structure and its transformations occurring at various length scales during plastic deformation. In addition, the deformation mechanisms may be different in different nanocrystalline materials or even in the same material at different conditions of loading (say, temperature, strain rate). In these circumstances, further theoretical and experimental investigations in this area are highly desired for understanding the fundamentals of the outstanding deformation behavior of nanocrystalline materials and development of high technologies exploiting their unique mechanical properties.

In conclusion of this review, let us outline the key points which are interesting for the future theoretical studies of plastic deformation processes and associated phenomena in nanocrystalline materials:

- 1) A theoretical description of new deformation mechanisms (in particular, rotation of nanograins) in nanocrystalline materials.
- 2) A theoretical description of the role of triple junctions and quadruple nodes of grain boundaries (which are treated as thermodynamically distinct phases, separate from grain boundaries and

grain interiors [137]) in deformation processes in nanocrystalline materials.

- (3) Development of the generalized model which will describe the combined action of different deformation mechanisms (such as lattice dislocation motion in grain interiors, grain boundary sliding, diffusion plasticity mechanisms associated with grain boundary diffusion and triple junction diffusion) whose contribution to plastic flow in nanocrystalline materials is dependent on the material characteristics, grain size distribution and conditions of loading.
- (4) A theoretical analysis of the specific features of plastic flow in nanocrystalline films and coatings where the residual stresses are capable of essentially influencing grain boundary structures (see, e.g., [7, 138, 139]) and deformation processes.
- (5) A theoretical analysis of the specific features of plastic flow in nanocomposite materials where the composite structure and interphase boundaries are capable of strongly affecting deformation processes.
- (6) A theoretical analysis of the influence of plastic deformation on the structural stability (against grain growth) in nanocrystalline materials.

## ACKNOWLEDGEMENTS.

This work was supported (for MYuG and IAO) by INTAS (grant 99-1216) and the Volkswagen Foundation (research project 05019225), and (for IAO) by the the Russian Foundation for Basic Researches (grant 01-02-16853), the Office of US Naval Research (grant N00014-01-1-1020), and the Office of US Naval Research, International Field Office Europe (grant N00014-00-1-4075), and (for CSP) by the Office of US Naval Research.

## REFERENCES

- [1] H. Gleiter // *Acta Mater.* **48** (2000) 1.
- [2] *Nanostructured Films and Coatings*, NATO Science Ser., ed. by G.-M. Chow, I.A. Ovid'ko and T. Tsakalakos (Kluwer, Dordrecht, 2000).
- [3] *Nanotechnology Research Directions*, ed. by M.C. Roco, R.S. Williams and P. Alivisatos (Kluwer, Dordrecht, 2000).
- [4] *Nanomaterials: Synthesis, Properties and Applications*, ed. by A.S. Edelstain and R.C. Camarata (Institute of Physics Publ., Bristol and Philadelphia, 1996).
- [5] *R&D Status and Trends in Nanoparticles, Nanostructured Materials, and Nanodevices in the United States*, ed. by R.W. Siegel, E. Hwu and M.C. Roco (International Technology Research Institute, Baltimore, 1997).
- [6] *Handbook of Nanostructured Materials and Nanotechnology*, Vol. 1-5, ed. by H.S. Nalwa (Academic Press, San Diego, 1999).
- [7] I.A. Ovid'ko // *Rev. Adv. Mater. Sci.* **1** (2000) 61.
- [8] V.A. Shchukin and D. Bimberg // *Rev. Mod. Phys.* **71** (1999) 1125.
- [9] N.N. Ledentsov, V.M. Ustinov, V.A. Shchukin, P.S. Kop'ev, Zh.I. Alferov and D. Bimberg // *Semiconductors* **32** (1998) 343.
- [10] M.Yu. Gutkin and I.A. Ovid'ko, *Defects and Plasticity Mechanisms in Nanostructured and Non-crystalline Materials* (St. Petersburg, Yanus, 2001), in Russian.
- [11] R.W. Siegel and G.E. Fougere // *Nanostruct. Mater.* **6** (1995) 205.
- [12] H. Hahn and K.A. Padmanabhan // *Nanostruct. Mater.* **6** (1995) 191.
- [13] H.W. Song, S.R. Guo and Z.Q. Hu // *Nanostruct. Mater.* **11** (1999) 203.
- [14] M.J. Mayo // *Nanostruct. Mater.* **9** (1997) 717.
- [15] M.J. Mayo, In: *Nanostructured Materials: Science and Technology*, ed. by G.-M. Chow and N.I. Noskova (Dordrecht, Kluwer, 1998), p. 361.
- [16] E.O. Hall // *Proc. Phys. Soc. London B* **64** (1951) 747.
- [17] N.J. Petch // *J. Iron Steel Inst.* **174** (1953) 25.
- [18] R. A. Masumura, P. M. Hazzledine and C. S. Pande // *Acta Mater.* **46** (1998) 4527.
- [19] C. S. Pande, R. A. Masumura and R. W. Armstrong // *Nanostruct. Mater.* **2** (1993) 323.
- [20] P.G. Sanders, J.A. Eastman and J.R. Weertman // *Acta Mater.* **45** (1997) 4019.
- [21] R.M. Christensen, *Mechanics of Composite Materials* (Wiley-Interscience, New York, 1979).
- [22] S. Nemat-Nasser and M. Hori, *Micromechanics: Overall Properties of Heterogeneous Materials* (Elsevier Publishers B.V., Amsterdam/London/New York/Tokyo, 1993).
- [23] U.F. Kocks // *Metal. Trans.* **1** (1970) 1121.
- [24] A. Lasalmonie and J.L. Strudel // *J. Mater. Sci.* **21** (1986) 1837.
- [25] J.S.C. Jang and C.C. Koch // *Scr. Metall. Mater.* **24** (1990) 1599.
- [26] V.G. Gryaznov, M.Yu. Gutkin, A.E. Romanov and L.I. Trusov // *J. Mater. Sci.* **28** (1993) 4359.

- [27] G.D. Hughes, S.D. Smith, C.S. Pande, H.R. Johnson and R.W. Armstrong // *Scr. Metall.* **20** (1986) 93.
- [28] K. Hayashi and H. Etoh // *Mater. Trans. Jpn. Inst. Metals* **30** (1989) 925.
- [29] R.W. Siegel, S. Ramasamy, H. Hahn, L. Zongquan, L. Ting and R. Gronsky // *J. Mater. Res.* **3** (1988) 1367.
- [30] R.W. Siegel, H. Hahn, S. Ramasamy, L. Zongquan, L. Ting and R. Gronsky // *J. Phys. Colloq.* **49** (1988) 681.
- [31] H.J. Höfler and R.S. Averback // *Scr. Metall. Mater.* **24** (1990) 2401.
- [32] A.H. Chokshi, A. Rosen, J. Karch and H. Gleiter // *Scr. Metall.* **23** (1989) 1679.
- [33] G.W. Nieman, J.R. Weertman and R.W. Siegel // *Scr. Metall.* **23** (1989) 2013.
- [34] G.W. Nieman, J.R. Weertman and R.W. Siegel // *J. Mater. Res.* **6** (1991) 1012.
- [35] D.G. Morris and M.A. Morris // *Acta Metall. Mater.* **39** (1991) 1763.
- [36] G.E. Fougere, J.R. Weertman and R.W. Siegel // *Nanostruct. Mater.* **5** (1995) 127.
- [37] N.P. Kobelev, Ya.M. Soifer, R.A. Andrievski and B. Gunther // *Nanostruct. Mater.* **2** (1993) 537.
- [38] X.Y. Qin, X.J. Wu and L.D. Zhang // *Nanostruct. Mater.* **5** (1995) 101.
- [39] T.D. Shen and C.C. Koch // *Nanostruct. Mater.* **5** (1995) 615.
- [40] T.R. Smith and K.S. Vecchio // *Nanostruct. Mater.* **5** (1995) 11.
- [41] X.D. Liu, Z.Q. Hu and B.Z. Ding // *Nanostruct. Mater.* **2** (1993) 545.
- [42] X.D. Liu, B.Z. Ding, Z.Q. Hu, K. Lu and Y.Z. Wang // *Physica B* **192** (1993) 345.
- [43] K. Lu, W.D. Wei and J.T. Wang // *Scr. Metall. Mater.* **24** (1990) 2319.
- [44] G. Palumbo, U. Erb and K.T. Aust // *Scr. Metall. Mater.* **24** (1990) 2347.
- [45] H. Chang, H.J. Höfler, C.J. Altstetter and R.S. Averback // *Scr. Metall. Mater.* **25** (1991) 1161.
- [46] T. Christman and M. Jain // *Scr. Metall. Mater.* **25** (1991) 767.
- [47] K. Kim and K. Okazaki // *Mater. Sci. Forum* **88-90** (1992) 553.
- [48] X. Zhu, R. Birringer, U. Herr and H. Gleiter // *Phys. Rev. B* **35** (1987) 9085.
- [49] E. Jorra, H. Franz, J. Peisl, G. Wallner, W. Petry, T. Haubold, R. Birringer and H. Gleiter // *Phil. Mag. B* **60** (1989) 159.
- [50] T. Haubold, R. Birringer, B. Lengeler and H. Gleiter // *Phys. Lett. A* **135** (1989) 461.
- [51] U. Herr, J. Jing, R. Birringer, U. Conser and H. Gleiter // *Appl. Phys. Lett.* **50** (1987) 472.
- [52] H.-E. Schaefer and R. Würshum // *Phys. Lett. A* **119** (1987) 370.
- [53] R. Würshum, M. Scheytt and H.-E. Schaefer // *Phys. stat. sol. (a)* **102** (1987) 119.
- [54] H.-E. Schaefer, R. Würschum, R. Birringer and H. Gleiter // *Phys. Rev. B* **38** (1988) 9545.
- [55] J. Friedel, *Dislocations*, (Pergamon Press, Oxford/London/Edinburgh/New York/Paris/Frankfurt, 1964).
- [56] H. Gleiter // *Progr. Mater. Sci.* **33** (1989) 223.
- [57] H. Gleiter // *Nanostruct. Mater.* **1** (1992) 1.
- [58] H. Gleiter // *Nanostruct. Mater.* **6** (1995) 3.
- [59] P.G. Cheremskoi, V.V. Slezov and V.I. Betekhtin, *Pores in Solid* (Energoatomizdat, Moscow, 1990), in Russian.
- [60] R.W. Armstrong // *Metall. Trans.* **1** (1970) 1169.
- [61] V.I. Trefilov, V.F. Moiseev and E.P. Pechkovskii, *Deformational Strengthening and Fracture of Polycrystalline Metals* (Naukova Dumka, Kiev, 1987), in Russian.
- [62] R.W. Armstrong, In: *Ultrafine-Grain Metals*, ed. by J.J. Burke and V. Weiss (Syracuse University Press, Syracuse, NY, 1972).
- [63] U. Erb, A.M. El-Sherik, G. Palumbo and K.T. Aust // *Nanostruct. Mater.* **2** (1993) 383.
- [64] N.I. Noskova, E.G. Ponomareva, I.A. Pereturina and V.N. Kuznetsov // *Phys. Met. Metallogr.* **81** (1996) 162.
- [65] N.I. Noskova, In: *The Structure, Phase Transformation and Properties of Nanocrystalline Alloys* (UD RAS, Ekaterinburg, 1997), p. 5, in Russian.
- [66] N.I. Noskova, In: *Nanostructured Materials: Science and Technology*, ed. by G.-M. Chow and N.I. Noskova (Kluwer Academic Publishers, Dordrecht/Boston/London, 1998), p. 93.
- [67] M. Yu. Gutkin and I.A. Ovid'ko // *Nanostruct. Mater.* **2** (1993) 631.
- [68] M. Yu. Gutkin and I.A. Ovid'ko, In: *Strength of Materials*, ed. by H. Oikawa, K. Maruyama, S. Takeuchi and M. Yamaguchi (The Japan Institute of Metals, Sendai, 1994), p. 227.
- [69] J.E. Carsley, J. Ning, W.W. Milligan, S.A. Hackney and E.C. Aifantis // *Nanostruct. Mater.* **5** (1995) 441.
- [70] H.S. Kim // *Scr. Mater.* **39** (1998) 1057.
- [71] D.A. Konstantinidis and E.C. Aifantis // *Nanostruct. Mater.* **10** (1998) 1111.
- [72] V.A. Jorin, V.B. Fedorov, D.K. Khakimova, E.G. Galkina, E.V. Tatianin and

- N.S.Enikolopian // *Soviet Phys. Dokl.* **275** (1984) 1447.
- [73] I.D.Morokhov, V.B.Fedorov, E.G.Galkina and E.V.Tatianin, In: *Physico-Chemistry of Ultra-Disperse Systems*, ed. by I.V.Tananaev (Nauka, Moscow, 1987), p. 157, in Russian.
- [74] A.M. Glezer, B.V. Molotilov, V.P. Ovcharov, O.L. Utevskaia and Yu.E. Chicherin // *Phys.Met.Metallogr.* **64** (1987) 1106.
- [75] I.A.Ovid'ko, *Defects in Condensed Media: Glasses, Crystals, Quasicrystals, Liquid Crystals, Magnetics, Superfluids* (Znanie, St.Petersburg, 1991), in Russian.
- [76] A.E.Romanov and V.I.Vladimirov, In: *Dislocations in Solids*, Vol.9, ed. by F.R.N.Nabarro (North-Holland, Amsterdam, 1992), p. 191.
- [77] V.A.Likhachev and V.E.Shudegov, *Principles of Organization of Amorphous Structures* (St.Petersburg State University, St.Petersburg, 1999), in Russian.
- [78] N. Rivier // *Adv. Phys.* **36** (1987) 95.
- [79] V.V.Rybin, *Large Plastic Deformations and Fracture of Metals* (Metallurgia, Moscow, 1986), in Russian.
- [80] M.Yu. Gutkin, I.A. Ovid'ko and A.E. Romanov // *Radiat. Eff. Def. Sol.* **129** (1994) 239.
- [81] G.S.Pisarenko, A.P.Yakovlev and V.V.Matveev, *Handbook on Strength of Materials* (Naukova Dumka, Kiev, 1988), in Russian.
- [82] D.Tabor, *The Hardness of Metals* (Oxford University Press, London, 1951).
- [83] R.C.Morris // *J. Appl. Phys.* **50** (1979) 3250.
- [84] C.-P.Chou, L.A.Davis and M.C.Narasimhan // *Scr. Metall.* **11** (1977) 417.
- [85] L.A.Davis, Y.T.Yeow and P.M.Anderson // *J. Appl. Phys.* **53** (1982) 4838.
- [86] A.M.El-Sherik, U.Erb, G.Palumbo and K.T.Aust // *Scr. Metall. Mater.* **27** (1992) 1185.
- [87] R.A.Jago and N.Hansen // *Acta Metall. Mater.* **34** (1986) 1711.
- [88] N.Behnood, R.M.Douthwaite and J.T.Evans // *Acta Metall. Mater.* **28** (1980) 1133.
- [89] G.E.Fougere, J.R.Weertman, R.W.Siegel and S.Kim // *Scr. Metall. Mater.* **26** (1992) 1879.
- [90] N.Wang, Z.Wang, K.T.Aust and U.Erb // *Acta Metall. Mater.* **43** (1995) 519.
- [91] T.G.Nieh and J.Wadsworth // *Scr. Metall. Mater.* **25** (1991) 955.
- [92] G.W.Nieman, J.R.Weertman and R.W.Siegel // *Nanostruct. Mater.* **1** (1992) 185.
- [93] J.R. Weertman // *Mater. Sci. Eng. A* **166** (1993) 161.
- [94] C.J.Youngdahl, P.G.Sanders, J.A.Eastman and J.R.Weertman // *Scr. Mater.* **37** (1997) 809.
- [95] H.S. Kim, Y. Estrin and M.B. Bush // *Acta Mater.* **48** (2000) 493.
- [96] I.A. Ovid'ko // *Nanostruct.Mater.* **7** (1997) 149.
- [97] I.A. Ovid'ko // *Mater. Sci. Eng. A* **280** (2000) 355.
- [98] Y. Estrin, In: *Unified Constitutive Laws of Plastic Deformation*, ed.by A.S. Krausz and K.Krausz (Academic Press, New York, 1996), p. 69.
- [99] P.G.Sanders, J.A.Eastman and J.R.Weertman, In: *Processing and Properties of Nanocrystalline Materials*, ed. by C. Suryanarayana, J. Singh and F.H.Froes (TMS, Warrendale, PA, 1996), p. 397.
- [100] R.Suryanarayana, C.A.Frey, S.M.L.Sastry, B.E.Waller, S.E.Bates and W.E.Buhro // *J. Mater. Res.* **11** (1996) 439.
- [101] J. C. M. Li and Y. T. Chou // *Met. Trans.* **1** (1970) 1145.
- [102] T. E. Mitchell, S. S. Hecker and R. L. Smialek // *Phys. Stat. Sol.* **11** (1965) 585.
- [103] R. W. Armstrong and A. K. Head // *Acta Met.* **13** (1965) 759.
- [104] C. S. Pande and R. A. Masumura // *Proc. of Sixth International Conf. On Fracture* (1984) 857.
- [105] N. Louat // *Acta Met.* **33** (1985) 59.
- [106] A. G. Evans and J. P. Hirth // *Scripta Metall. Mater.* **26** (1992) 1675.
- [107] C. S. Pande and R. A. Masumura, In: *Processing and Properties of Nanocrystalline Materials*, ed. by C. Suryanarayana, J. Singh and F. H. Froes. (TMS, Warrendale, PA, 1996) 387.
- [108] Y.T. Chou // *J. Appl. Phys.* **38** (1967) 2080.
- [109] R.Z. Valiev, E. V. Kozlov, Yu. F. Inanov, J.Lian, A.A. Nazarov and B.Brandelet // *Acta Mater.* **42** (1994) 2467.
- [110] G.A. Malygin // *Phys. Solid State* **37** (1995) 1248.
- [111] J.C.M. Li // *Trans. TMS-AIME* **227** (1963) 247.
- [112] A.G. Evans and J.P. Hirth // *Scripta Metall.* **26** (1992) 1675.
- [113] K. Lu and M.L. Sui // *Scripta Metall. Mater.* **28** (1993) 1465.
- [114] R.O. Seattergood and C.C. Koch // *Scripta Mater.* **27** (1992) 1195.

- [115] A.A. Nazarov, A.E. Romanov, R.Z. Valiev and B. Baudelet // *Strength of Materials* (Japan, JIMIS, 1994) p. 877-879.
- [116] A.A. Nazarov // *Scripta Mater.* **34** (1996) 697.
- [117] J. Lian, B. Baudelet and A.A. Nazarov // *Mater. Sci. Eng. A* **172** (1993) 23.
- [118] S.G. Zaichenko and A.M. Glezer // *Phys. Sol. State* **39** (1997).
- [119] V.G. Gryaznov, A.M. Kaprelov and A.E. Romanov // *Scripta Metall.* **23** (1989) 1443.
- [120] V.G. Gryaznov, I.A. Polonsky, A.E. Romanov and L.I. Trusov // *Phys.Rev. B* **44** (1991) 42.
- [121] A.E. Romanov // *Nanostruct. Mater.* **6** (1995) 125.
- [122] R.W. Siegel, In: *Encycl. of Appl. Physics*, vol. 11, ed. by G.L. Trigg (VCH, Weinheim, 1994) p. 1.
- [123] H. Hahn, P. Mondal and K.A. Padmanabhan // *Nanostruct. Mater.* **9** (1997) 603.
- [124] V.V. Astanin, A.V. Sisanbaev, A.I. Pshenichnyuk and O.A. Kaibyshev // *Scripta Mater.* **36** (1997) 117.
- [125] H. Van Swygenhoven, M. Spavzer, A. Caro and D. Farkas // *Phys. Rev. B* **60** (1999) 22.
- [126] H. Van Swygenhoven, M. Spavzer and A. Caro // *Acta Mater.* **47** (1999) 3117.
- [127] I.A. Ovid'ko, submitted.
- [128] J.J. Gilman // *J. Appl. Phys.* **44** (1973) 675.
- [129] J.J. Gilman // *J. Appl. Phys.* **46** (1975) 1625.
- [130] I.A. Ovid'ko // *Phil. Mag.* **59** (1989) 523.
- [131] R.A. Andrievskii, G.V. Kalinnikov, N.P. Kobelev, Ya.M. Soifer and D.V. Shtansky // *Phys. Solid State* **39** (1997) 1661.
- [132] R.A. Andrievskii, In: *Nanostructured Materials: Science and Technology* (Kluwer Academic Publ., Dordrecht, 1998).
- [133] B. Burton // *Mat. Sci. Eng.* **10** (1972) 9.
- [134] S.M.L. Sastry, private communication, 1997.
- [135] K.J. Kurzydowski // *Scripta Metall. Mater.* **24** (1990) 879.
- [136] G. MacHahon and U. Erb // *Microstruct. Sci.* **17** (1989) 447.
- [137] A.H. King // *Interf. Sci.* **7** (1999) 251.
- [138] I.A. Ovid'ko and A.G. Sheinerman // *J. Nanosci. Nanotechnol.* **1** (2001) 215.
- [139] I.A. Ovid'ko // *J. Phys.: Condens. Matter.* **13** (2001) L97.